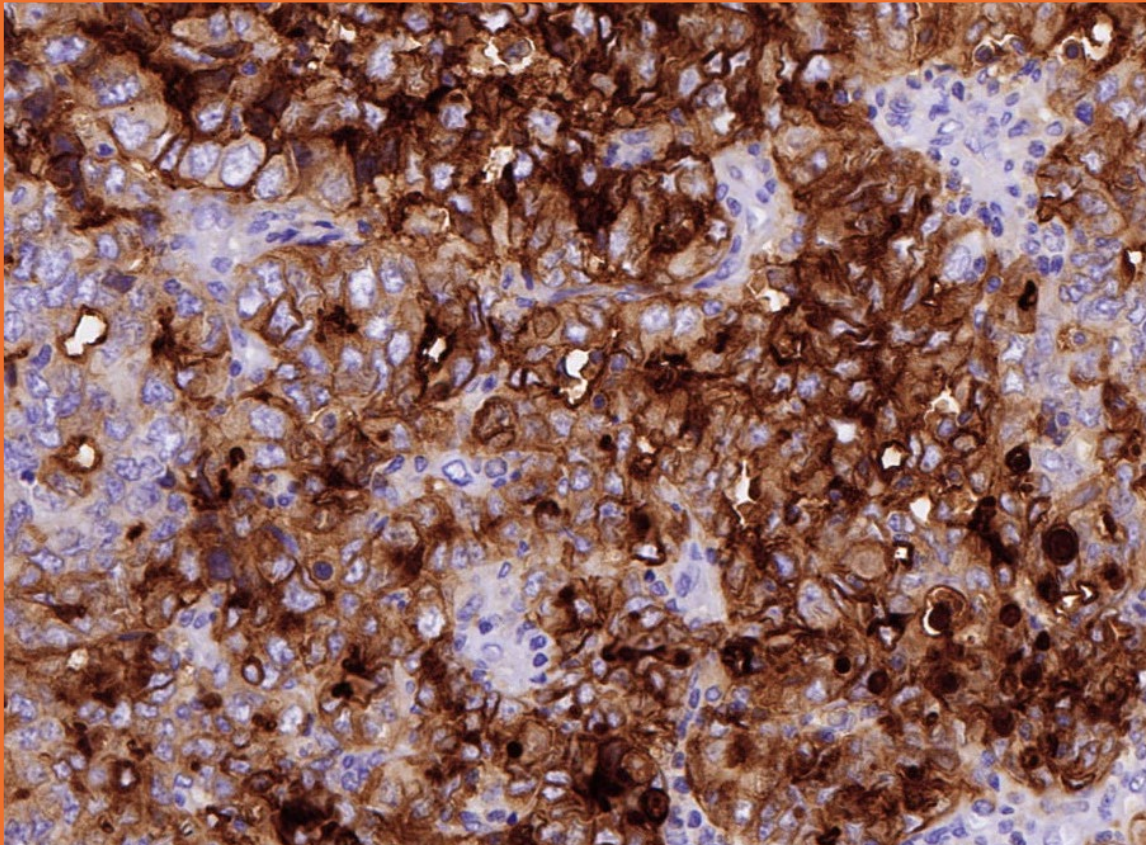


Enhanced validation data

Anti-folate binding protein/ FBP – ab221543



Folate binding protein expression in ovarian carcinoma

Enhanced validation of anti-folate binding protein/FBP recombinant antibody [EPR20277] – ab221543

Enhanced validation designed for your needs

We understand the challenge of finding the right antibody clone – highly specific and sensitive to your intended target – at early selection stages of your development program. To de-risk this clone selection process for you, we generated enhanced validation data for our best recombinant antibody clones to some of the most promising targets.

Our enhanced validation gives you an extra level of confidence in an antibody clone

- Provides additional data on the specificity and sensitivity of our recombinant antibodies in immunohistochemistry (IHC) and other relevant techniques
- Carried out in a custom manner, specific both to the target and the relevant research and clinical settings
- Builds upon our high-quality standard validation

Our framework for enhanced validation

- Our enhanced validation focuses on generating detailed IHC expression profiles for promising oncology targets in selected formalin-fixed paraffin-embedded (FFPE) human normal tissues and cancer tissue microarrays (TMAs).
- In this study, we demonstrate the sensitivity and specificity of anti-folate binding protein/FBP (ab221543) in knock-out cell lines and selected tissues and TMAs by IHC using a BOND™ RX Research Stainer (Leica®) and Ventana DISCOVERY ULTRA system (Roche Diagnostics).
- A quantitative H-score analysis of FBP expression was performed using the artificial intelligence (AI)-driven digital image analysis software Visiopharm® (Visiopharm A/S).

Leica® is a registered trademark of Leica Microsystems IR GmbH.
BOND™ is a trademark of Leica Biosystems Melbourne Pty. Ltd.
Visiopharm® is a registered trademark of Visiopharm A/S.

Enhanced validation data

Target overview

HGNC symbol

FOLR1

Approved name

Folate receptor alpha

Alternative names

Folate binding protein

FBP

Chromosomal location

11q13.4

Function

Folate binding protein binds folates on the cell surface and transports them via a receptor mediated endocytosis.¹

Tissue specificity

Folate binding protein is expressed in a few specific tissues, mainly on the membrane of certain epithelial tissues, like those in the kidney, lungs, and female reproductive organs.² It is often overexpressed in epithelial cancers, especially ovarian, uterine. lung cancers and is a therapeutic target of interest.²⁻⁷

Cellular localization

Membrane; secreted

Database links

[Entrez Gene: 2348](#)

[OMIM®: 136430](#)

[Uniprot: P15328](#)

Materials and methods

Human tissues were selected based on the target's expression and its current relevance to ongoing research and clinical trials. Gene expression was further analyzed for oncology targets in cBioPortal for Cancer Genomics using the Cancer Genome Atlas (TCGA) PanCancer Atlas datasets⁸⁻¹¹.

Tissue microarray (TMA)	Cores	Cases	Normal/ Benign cases	Cancer cases	Source (#catalog number)
Multi-normal ^(a)	15	15	15	0	In-house TMA
Multi-cancer ^(b)	35	35	1	34	In-house TMA
Ovarian cancer	102	102	5	97	Quickarrays (#OVC1021)
Lung cancer	102	102	5	97	Quickarrays (#LUC1021)

Table 1. List of human TMAs used in the enhanced validation. All tissues were sourced from Abcam-approved tissue suppliers.

a) The multi-normal TMA consists of the following tissues from one donors: colon, cerebrum, tonsil, stomach, testis, prostate, lung, skeletal muscle, heart, skin, spleen, pancreas, kidney, placenta and liver.

b) The multi-cancer TMA consists of the following tissues from two donors: seminoma, prostate adenocarcinoma, bladder carcinoma, renal cell carcinoma, melanoma, stomach adenocarcinoma, pancreatic adenocarcinoma, hepatocellular carcinoma, ovaria carcinoma, cervical cancer, head and neck carcinoma and endometrial cancer. The following tissues were from single donors: lung (squamous cell carcinoma (SCLC) and non-squamous cell carcinoma (NSCLC)), colon (adenocarcinoma and invasive adenocarcinoma), breast (ductal carcinoma and invasive lobular carcinoma), B cell lymphoma, T cell lymphoma, gliomas (grade II and IV) and placenta.

Step	Reagents	Method
Deparaffinization	DISCOVERY Wash (RUO)	Standard
Cell conditioning	ULTRA Cell Conditioning Solution (ULTRA CC1)	32 min, 100 °C
Pre-primary peroxidase inhibitor	OptiView Peroxidase Inhibitor	4 min
Primary antibody	Anti-folate binding protein recombinant antibody [EPR20277] – ab221543 diluted in Discovery Antibody Diluent (#760-108) to a final concentration of 0.5 µg/mL	16 min, 37 °C
Counterstain	Hematoxylin II	8 min
Post counterstain	Bluing Reagent	4 min

Table 2. IHC staining protocol on the Ventana DISCOVERY ULTRA (Roche Diagnostics) instrument. Staining was performed using standard conditions with OptiView DAB IHC Detection kit (#760-700).

Enhanced validation data

Step	Reagents	Method
Dewax	Bond™ dewax solution (AR922), alcohol, BOND wash solution (AR9590)	Dewax
Antigen retrieval	Bond™ epitope retrieval ER2 solution (AR9640)	HIER with ER2 (pH 9.0), 20 min, 100°C

Step	Reagents	Number of washes	Time (minutes)
Peroxide block	3-4% (v/v) Hydrogen peroxide	-	5
Wash	Bond™ wash solution	3x	0
Primary antibody	Anti-folate binding protein recombinant antibody [EPR20277] – ab221543 diluted in Bond™ primary antibody diluent (#AR9352) to final concentration of 0.3 µg/mL	-	15
Wash	Bond™ wash solution	4x	0
Secondary antibody	Bond™ polymer refine detection (DS9800)	-	8
Wash	Bond™ wash solution	2x	4
	Deionized water	1x	0
Visualization	Mixed DAB refine (DS9800)	1x	0
	Mixed DAB refine (DS9800)	-	10
Wash	Deionized water	3x	0
Counterstain	Hematoxylin (DS9800)	-	5
Wash	Deionized water	1x	0
	Bond™ wash solution	1x	0
	Deionized water	1x	0

Table 3. IHC staining protocol on BOND™ RX Research Stainer (Leica®). The protocol used is the same as the default IHC protocol F on BOND™ RX Research Stainer (Leica®), apart from the standard post-primary step, which has been excluded from our protocol. All steps were performed at room temperature.

H-score analysis

A quantitative H-score analysis of CD47 expression was performed using the artificial intelligence (AI)-driven digital image analysis software Visiopharm® (Version: 2023.09). TMA slides were de-arrayed and the tissue within each core was detected. Tissue detection, artefact exclusion and segmentation were performed using models with DeepLabv3+ architecture.

Total cell numbers for each core were counted using a trained AI model with U-Net architecture. Using the cell analysis data and thresholds, cell membrane H-scores of tumor cells in the TMAs were calculated in Visiopharm® and the graphical representation was generated using GraphPad Prism 10.

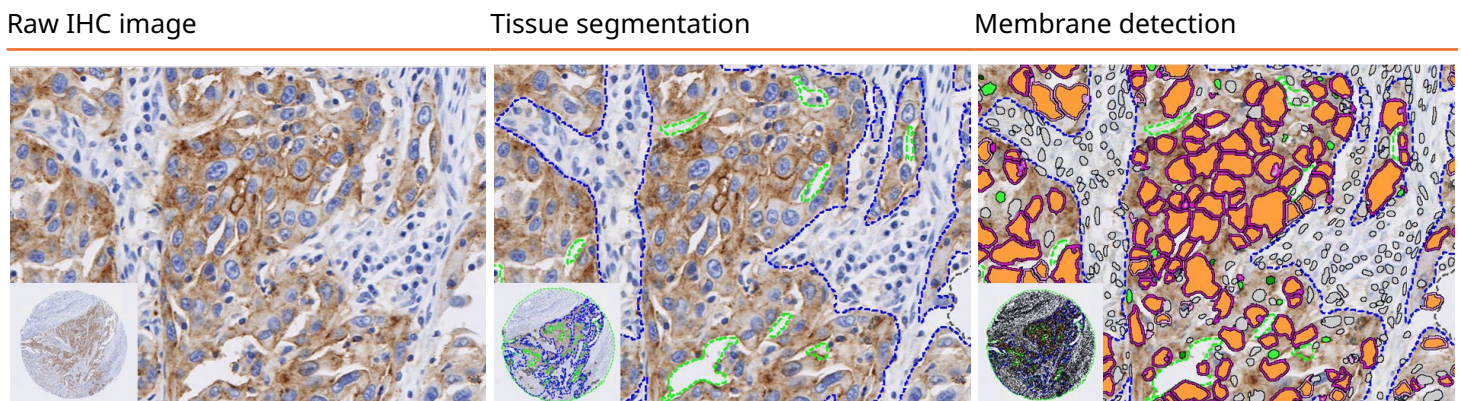


Figure 1. Visiopharm® tissue segmentation and membrane detection. Raw IHC images were subjected to total cell detection to determine staining intensity. There are four intensity scores shown in the example here: gray (0), pink (1+), magenta (2+) and purple (3+). Areas in orange are irrelevant to these analyses.

IHC staining	Corresponding intensity score	Visiopharm® intensity threshold
Negative	0	> 255
Weak	1+	< 255
Moderate	2+	< 190
Strong	3+	< 160

Table 4. Intensity scoring and thresholds for H-score analysis. The H-score captures both the IHC staining intensity and the percentage of stained cells at each intensity level. It was calculated using the formula $H\text{-score} = [(0 \times \% \text{ of negative cells}) + (1 \times \% \text{ of weak stained cells}) + (2 \times \% \text{ of moderate stained cells}) + (3 \times \% \text{ of strong stained cells})]$, giving an analytical range from 0 to 300.

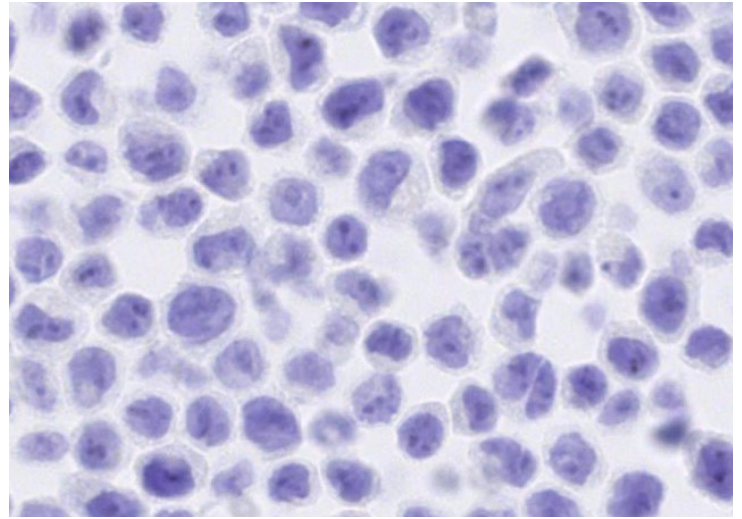
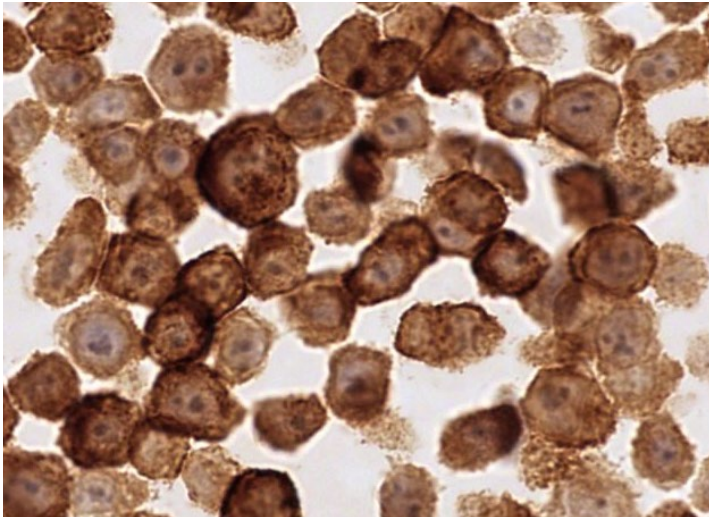
Folate binding protein expression in cell lines (BOND™ RX)

Below are representative images of folate binding protein expression in *FOLR1* wild-type and knock-out FFPE HeLa cells (ab264921). Folate binding protein was detected in the wild-type cell line but absent in the knock-out cell line.

HeLa *FOLR1* wild-type

HeLa *FOLR1* knock-out

FBP



Isotype control

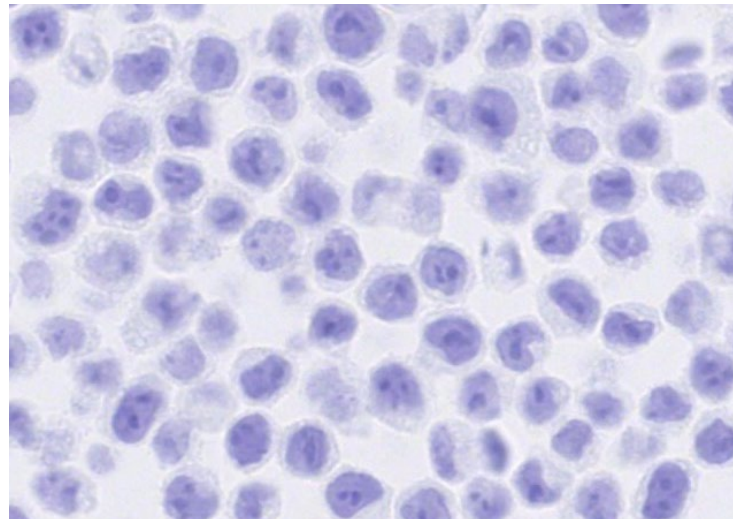
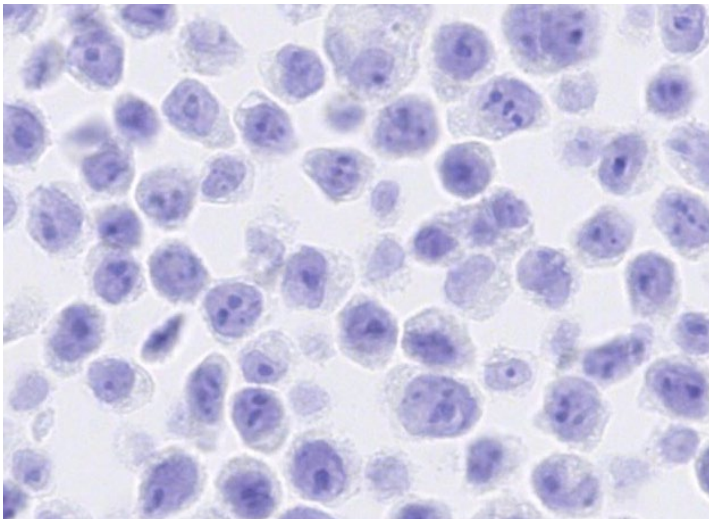


Figure 2. Folate binding protein expression in *FOLR1* wild-type and knock-out HeLa cell lines. IHC staining of FFPE cell pellets using anti-folate binding protein (ab221543) (0.3ug/mL) or anti-rabbit IgG-isotype control antibody (1.0 µg/mL) (ab172730). Positive staining in brown; nuclear hematoxylin counterstain in blue. Slides were stained using a BOND™ RX Research Stainer (Leica®), scanned at 20x on NanoZoomer® S360 (Hamamatsu Photonics K.K.) and imaged at 40X on Aperio® ImageScope.

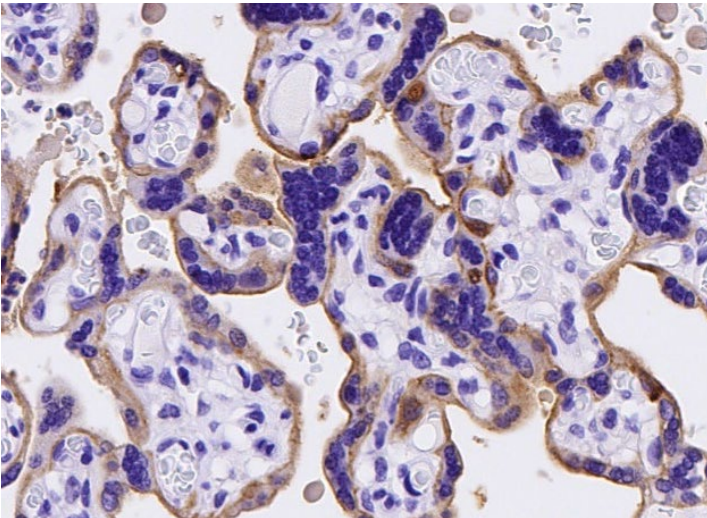
NanoZoomer® is a registered trademark of Hamamatsu Photonics K.K.

For more information, please [contact us](#).

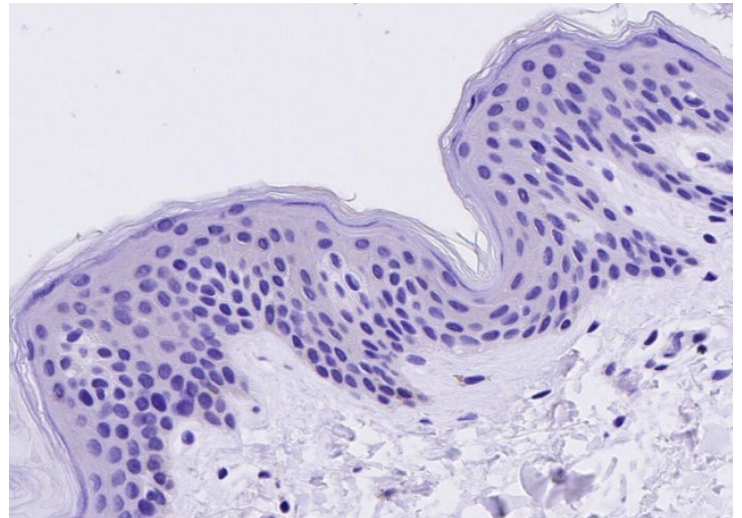
Folate binding protein expression in multi-normal TMA (BOND™ RX)

Below are the representative images of selected tissues from the multi-normal TMA. Folate binding protein expression was detected in the placenta, kidney and lung, whereas no expression was observed in the skin, testis, prostate, tonsil, skeletal muscle, heart, colon and cerebrum.

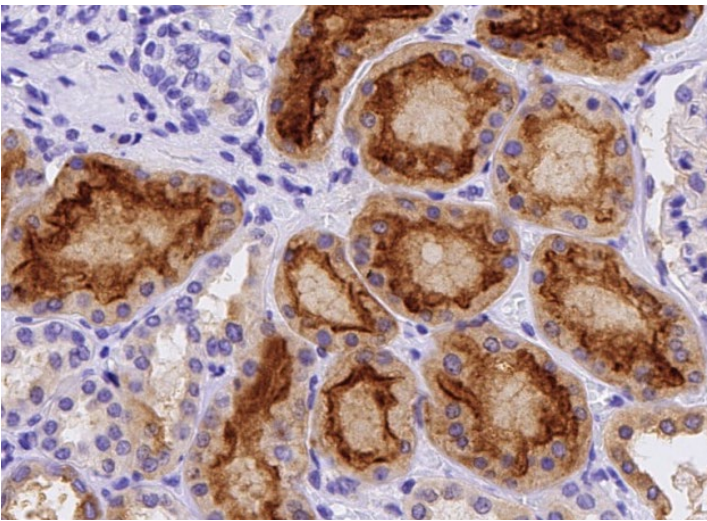
Placenta



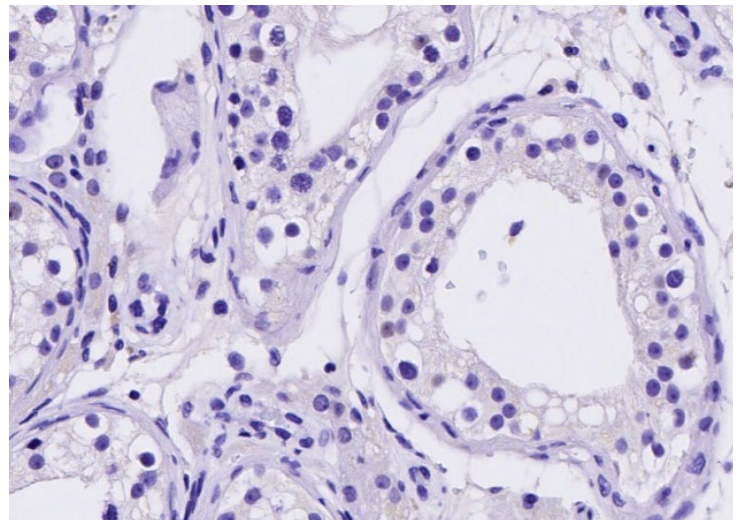
Skin



Kidney

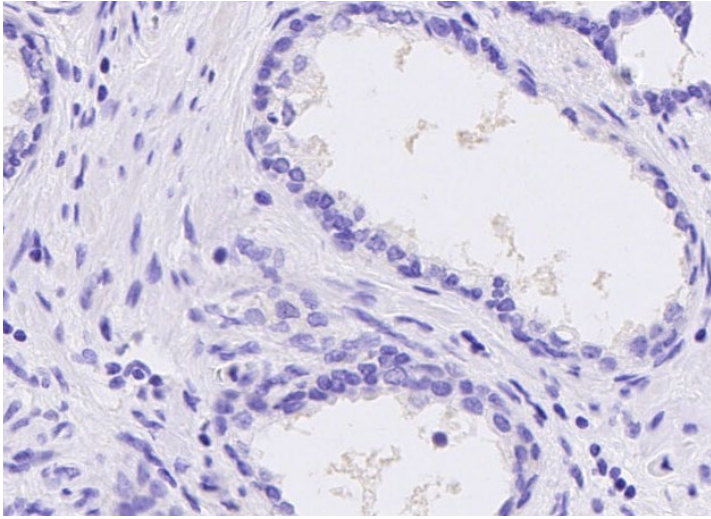


Testis

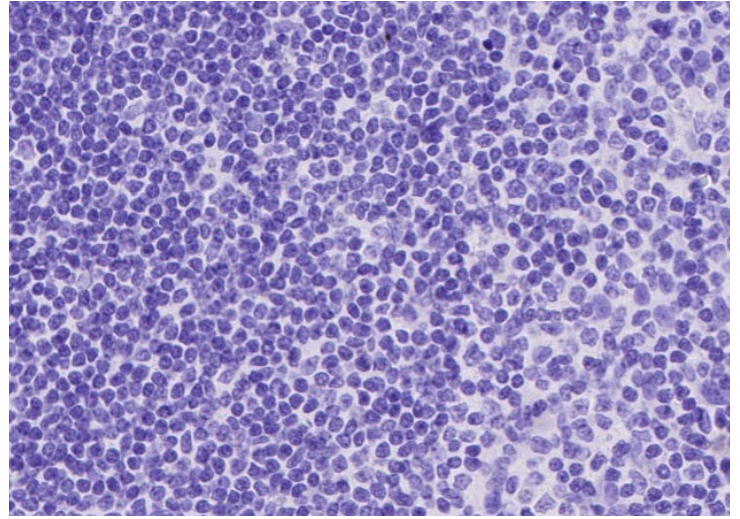


Enhanced validation data

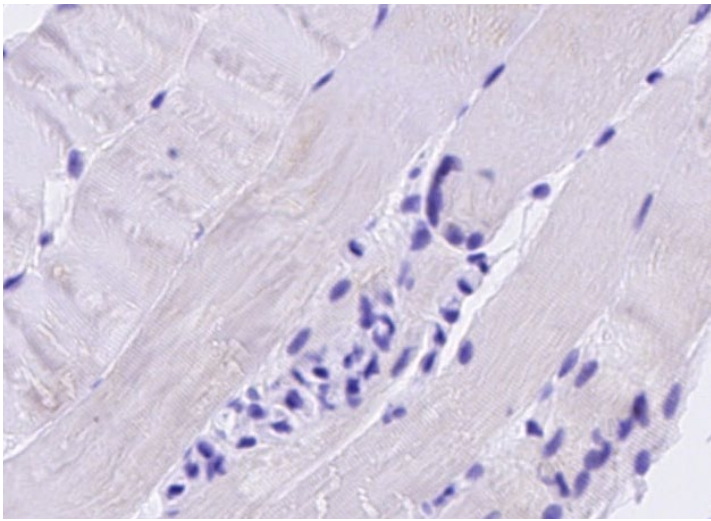
Prostate



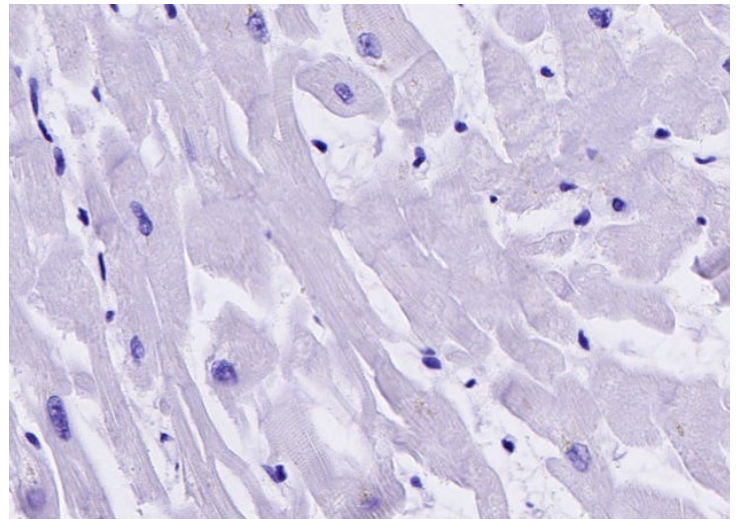
Tonsil



Skeletal muscle

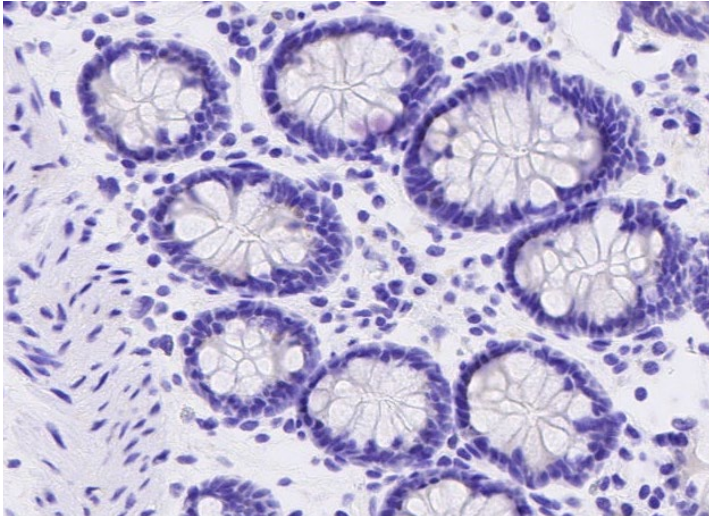


Heart

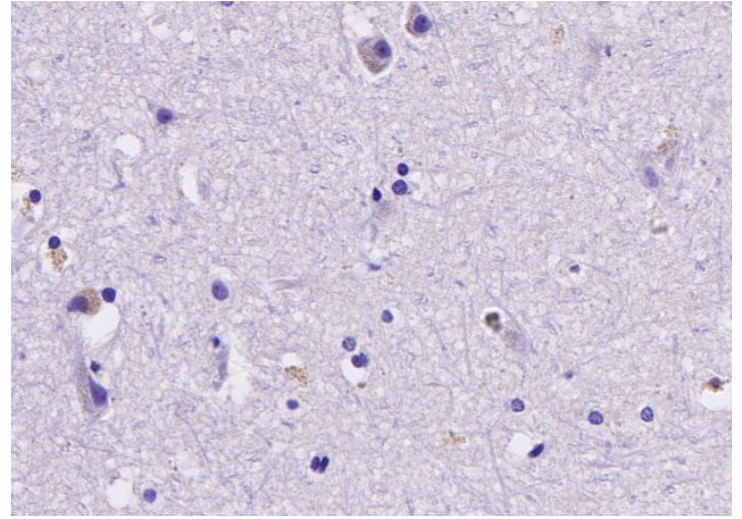


Enhanced validation data

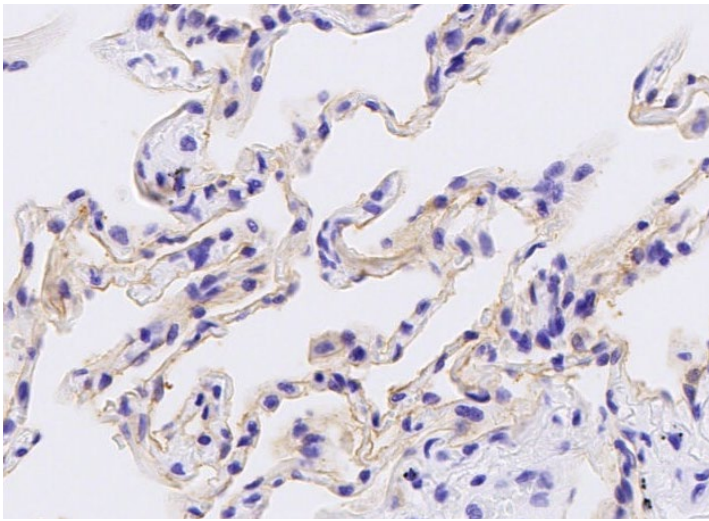
Colon



Cerebrum



Lung



Lung (isotype control)

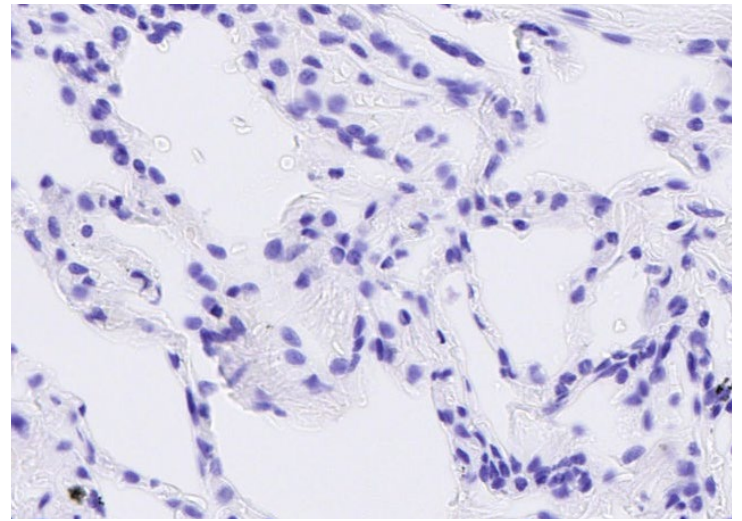
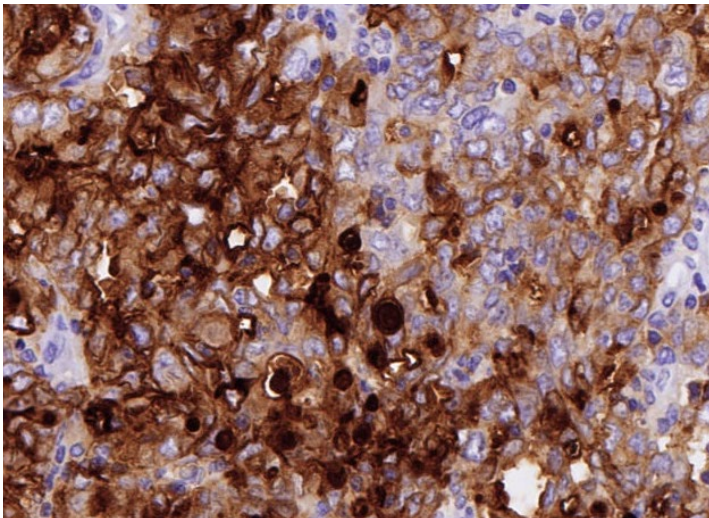


Figure 3. Folate binding protein expression in human normal tissue. IHC staining of multi-normal human tissues using anti-folate binding protein (ab221543) (0.3ug/mL) or anti-rabbit IgG-isotype control antibody (1.0 µg/mL) (ab172730). Positive staining in brown; nuclear hematoxylin counterstain in blue. Slides were stained using a BOND™ RX Research Stainer (Leica®), scanned at 20x on NanoZoomer® S360 and imaged at 20X on Aperio® ImageScope.

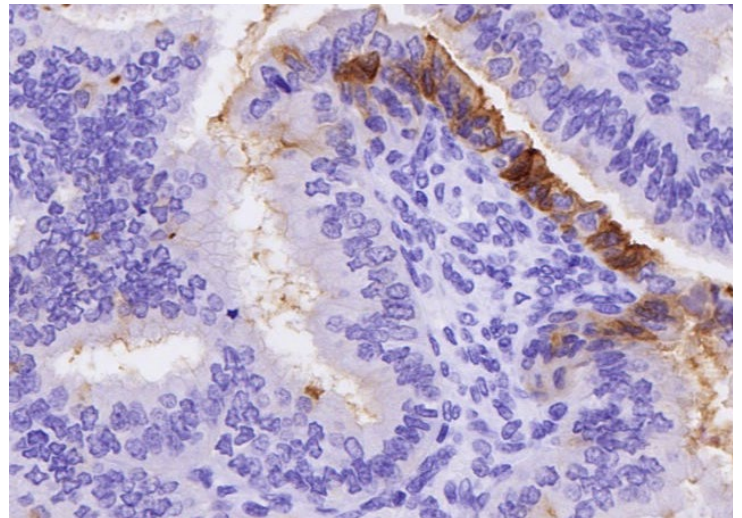
Folate binding protein expression in multi-cancer TMA (BOND™ RX)

Below are the representative images of selected tissues from the multi-cancer TMA. Folate binding protein expression was detected in ovarian carcinoma, endometrial carcinoma, lung adenocarcinoma, lung squamous cell carcinoma, stomach adenocarcinoma and glioblastoma. Expression was absent from breast lobular carcinoma, T cell lymphoma, seminoma, renal cell carcinoma and bladder carcinoma.

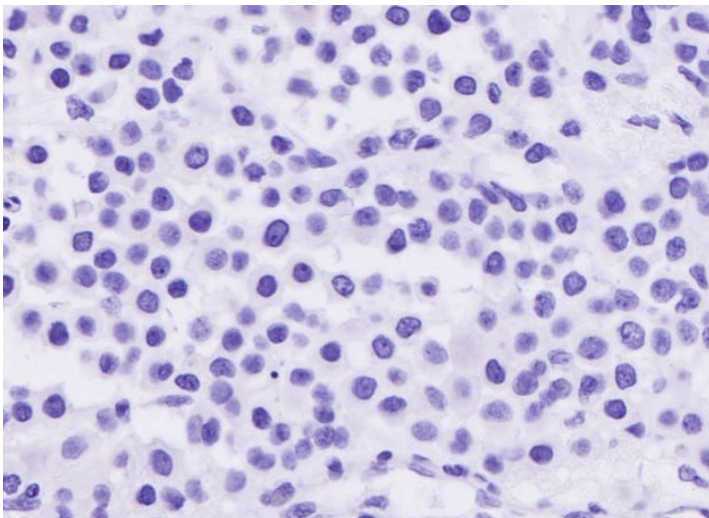
Ovarian carcinoma



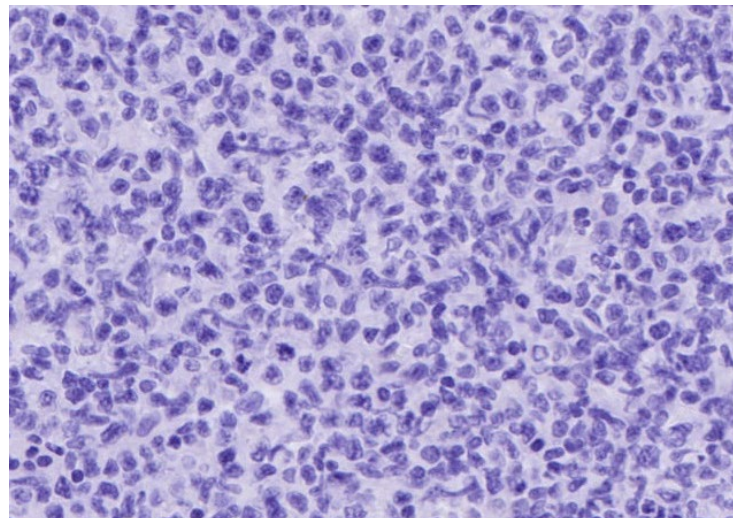
Endometrial carcinoma



Breast lobular carcinoma

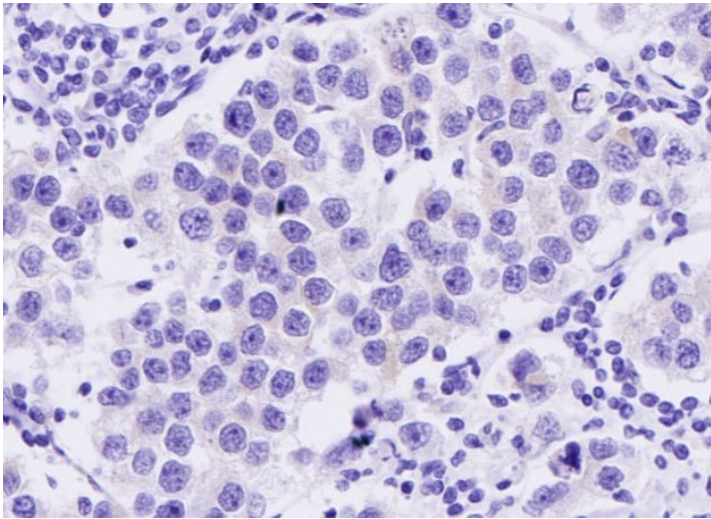


T cell lymphoma

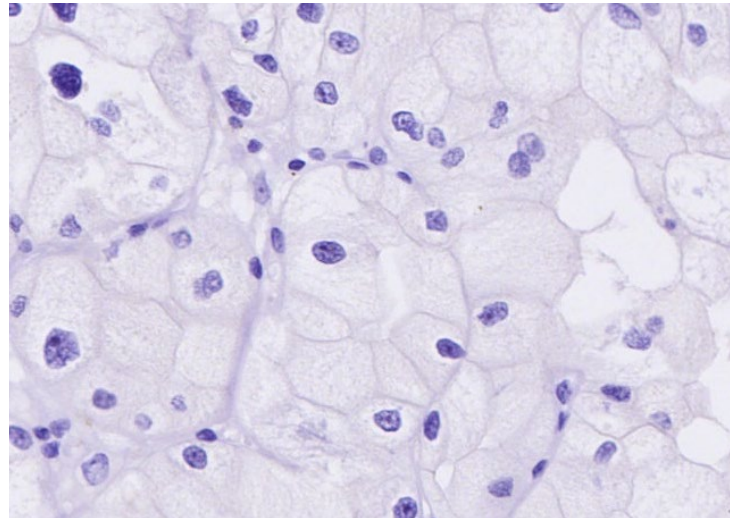


Enhanced validation data

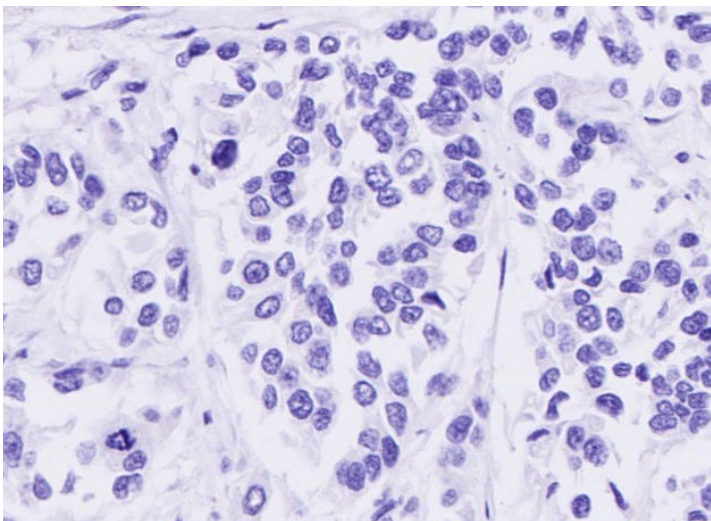
Seminoma



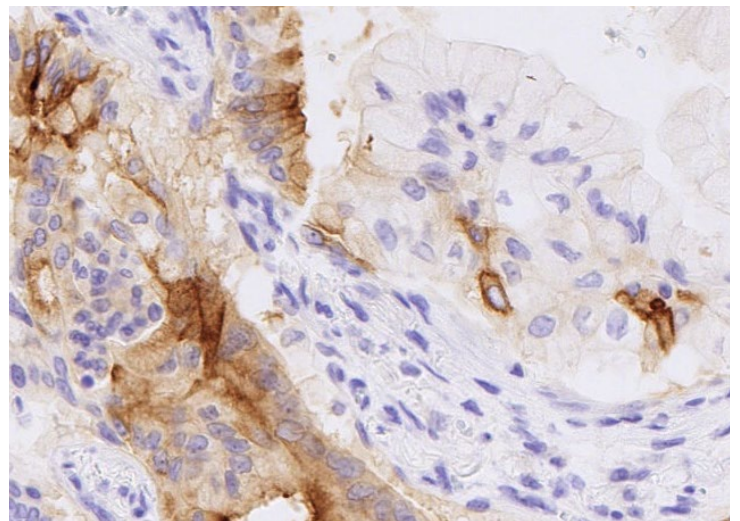
Renal cell carcinoma



Bladder carcinoma

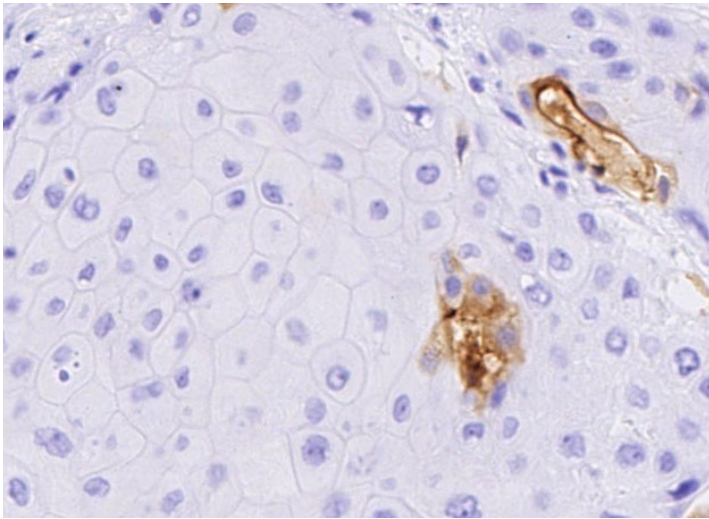


Lung adenocarcinoma

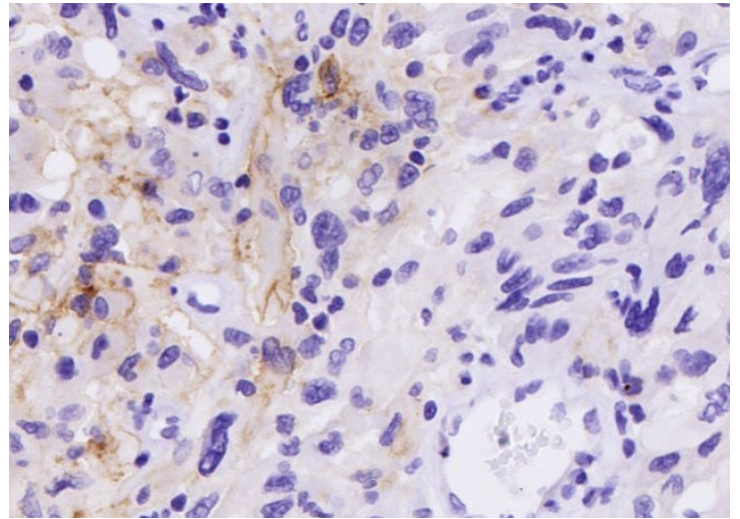


Enhanced validation data

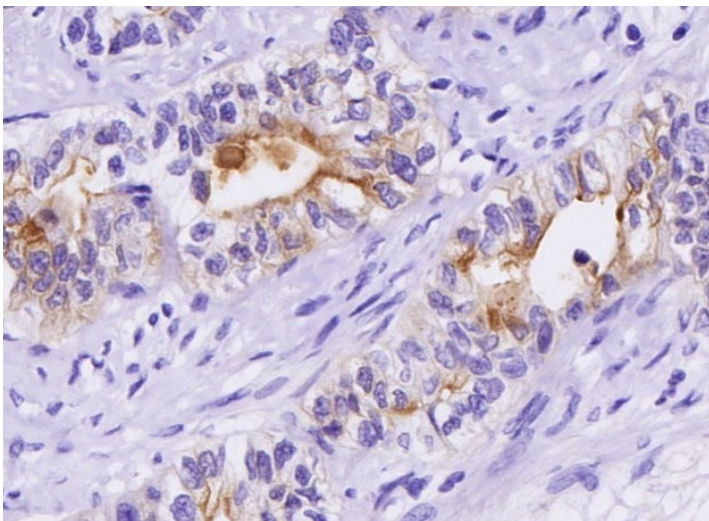
Lung squamous cell carcinoma



Glioblastoma



Stomach adenocarcinoma



Pancreas adenocarcinoma

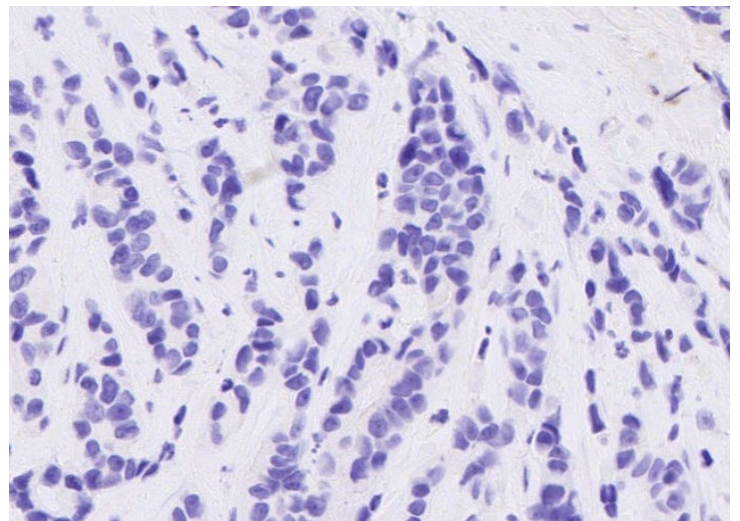
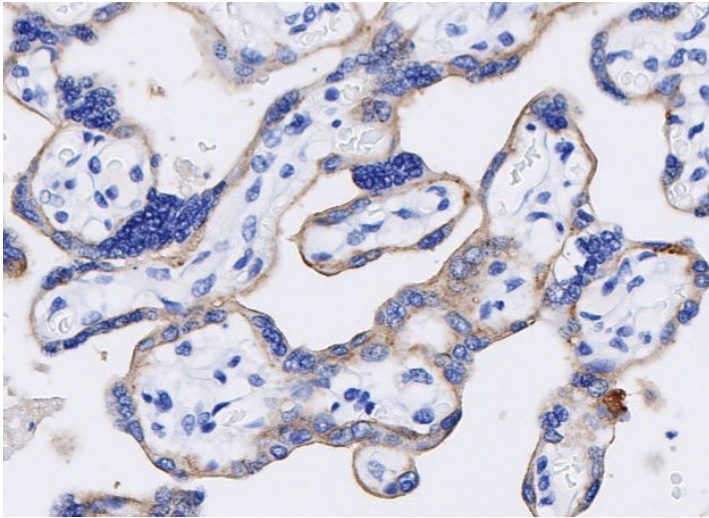


Figure 4. Folate binding protein expression in cancer. IHC staining of multi-cancer human tissues using anti-folate binding protein (ab221543) (0.3ug/mL) or anti-rabbit IgG-isotype control antibody (1.0 µg/mL) (ab172730). Positive staining in brown; nuclear hematoxylin counterstain in blue. Slides were stained using a BOND™ RX Research Stainer (Leica®), scanned at 20x on NanoZoomer® S360 and imaged at 20X on Aperio® ImageScope.

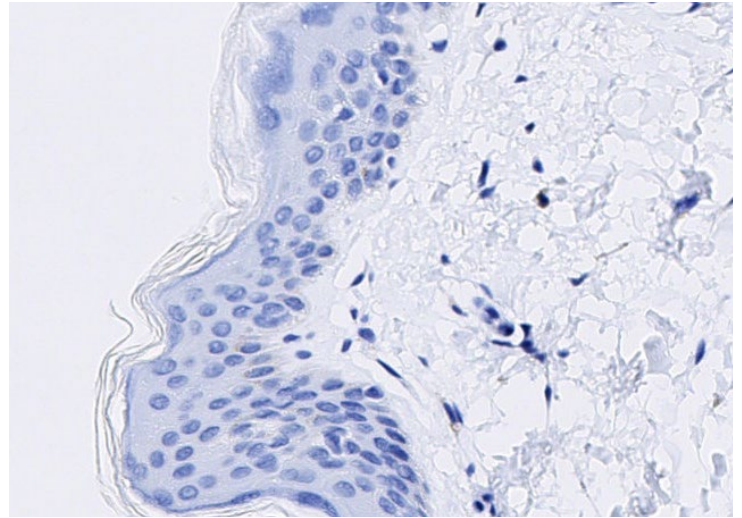
Folate binding protein expression in multi-normal TMA (DISCOVERY ULTRA)

Below are the representative images of selected tissues from the multi-normal TMA. Folate binding protein expression was detected in the placenta, kidney, whereas no expression was observed in the skin, skeletal muscle, testis, prostate, tonsil, spleen, heart, colon and stomach.

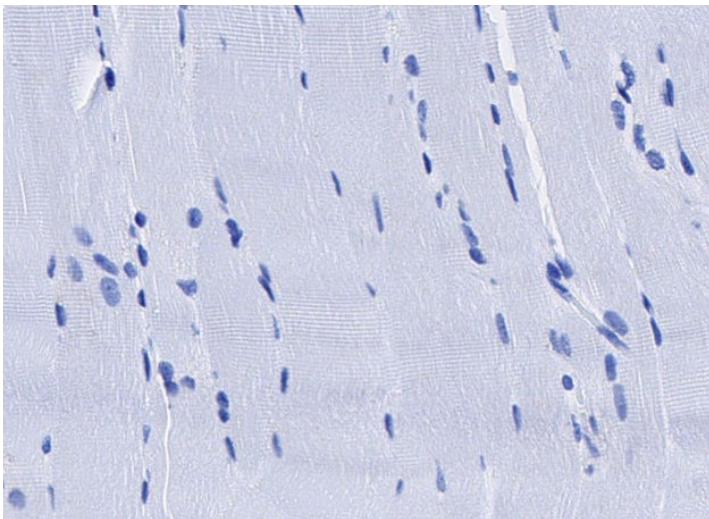
Placenta



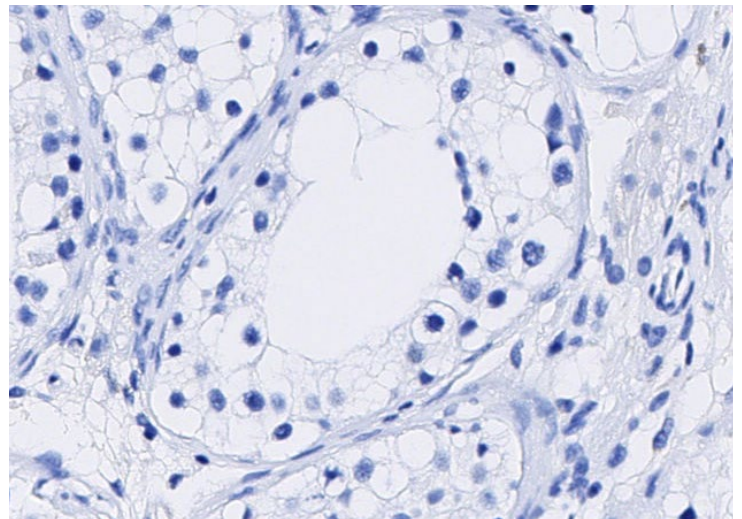
Skin



Skeletal muscle

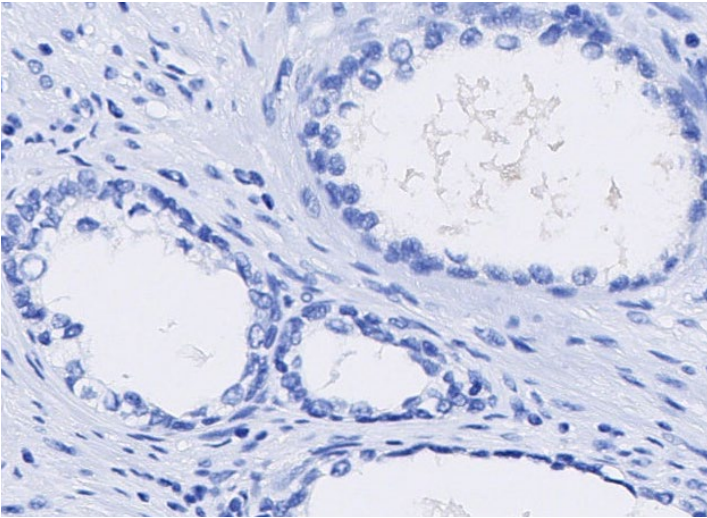


Testis

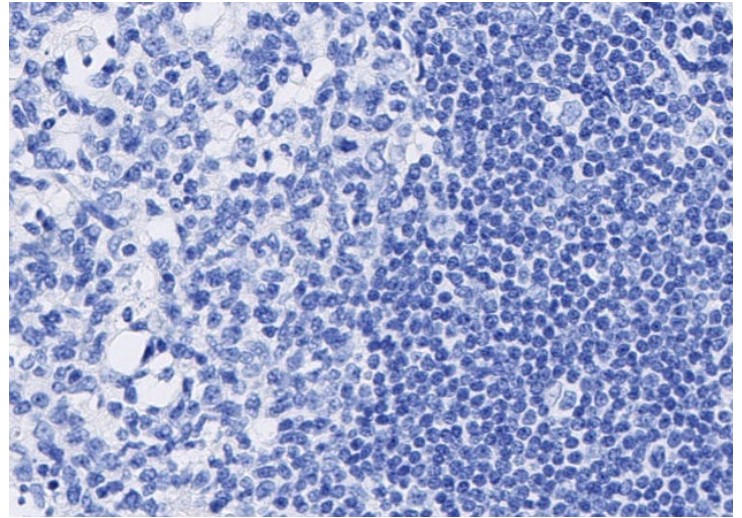


Enhanced validation data

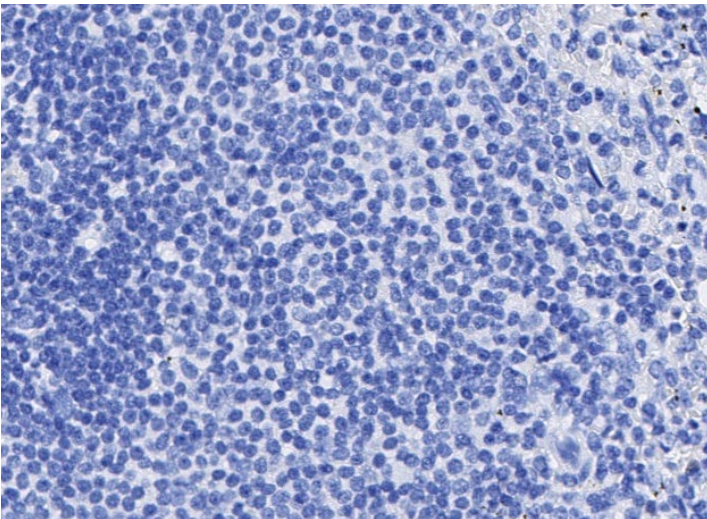
Prostate



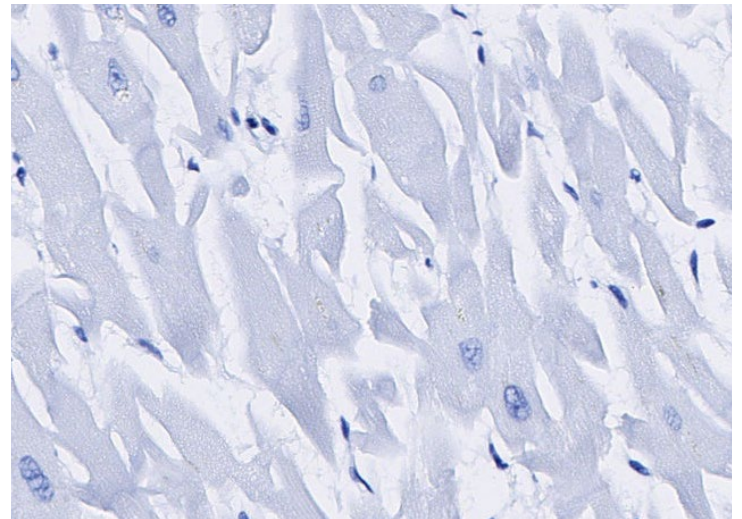
Tonsil



Spleen

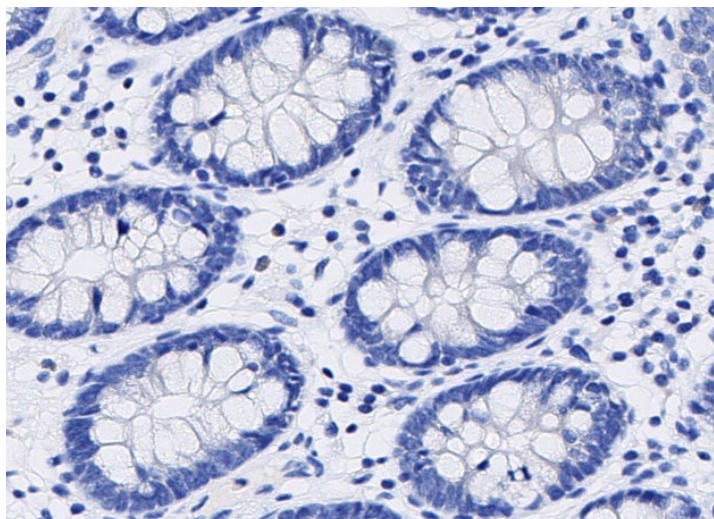


Heart

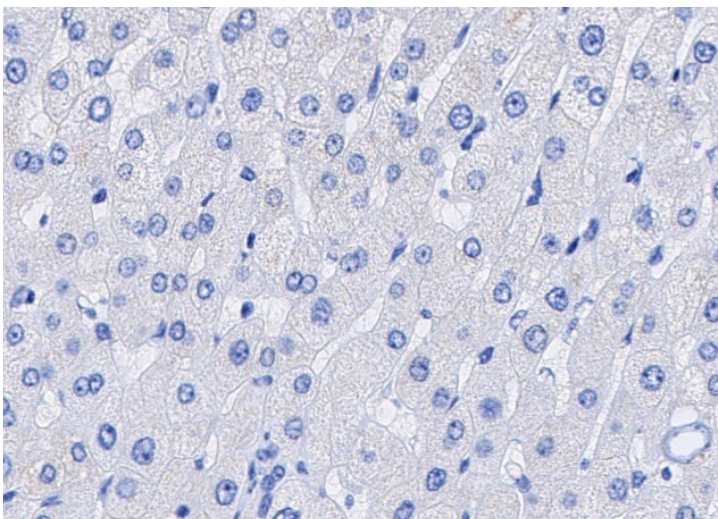


Enhanced validation data

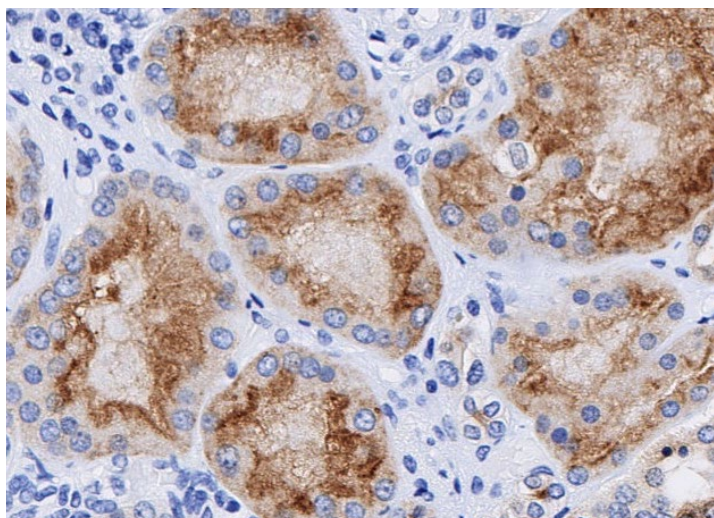
Colon



Stomach



Kidney



Kidney (isotype control)

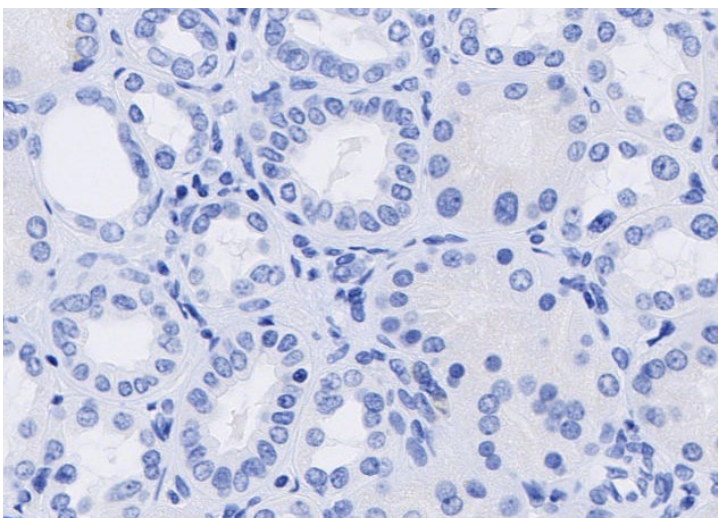
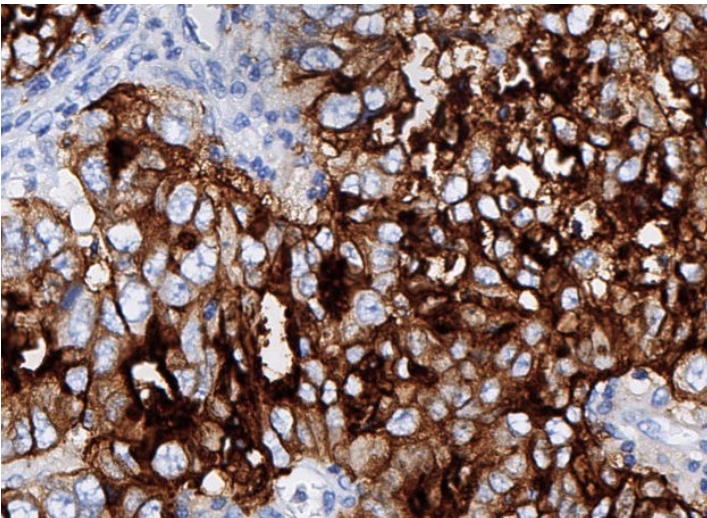


Figure 5. Folate binding protein expression in human normal tissue. IHC staining of multi-normal human tissues using anti-folate binding protein (ab221543) (0.5ug/mL) or anti-rabbit IgG-isotype control antibody (1.0 µg/mL) (ab172730) on the Ventana DISCOVERY ULTRA platform. Positive staining in brown; nuclear hematoxylin counterstain in blue. Slides were scanned at 20x on NanoZoomer® S360 and imaged at 20X on Aperio® ImageScope.

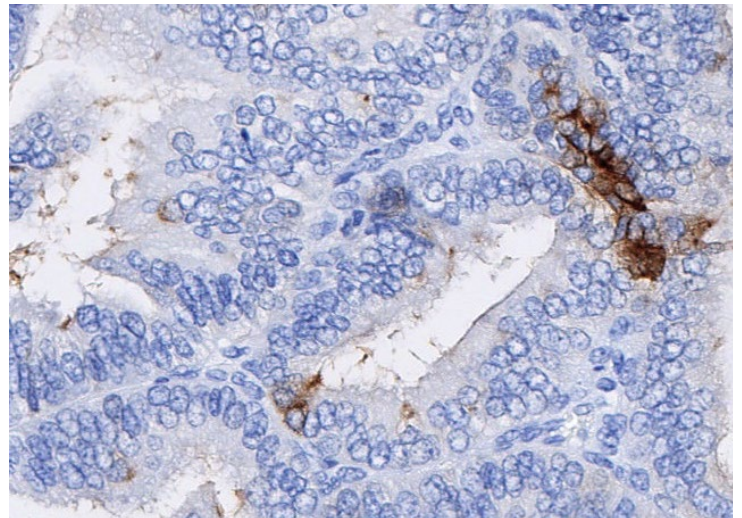
Folate binding protein expression in multi-cancer TMA (DISCOVERY ULTRA)

Below are the representative images of selected tissues from multi-cancer TMA. Folate binding protein expression was detected in carcinoma of the ovary, endometrium and lung, cervical cancer, adenocarcinoma of the lung and stomach, lung squamous cell carcinoma and glioblastoma. No expression was detected in breast lobular carcinoma, T cell lymphoma, seminoma, renal cell carcinoma or prostate adenocarcinoma.

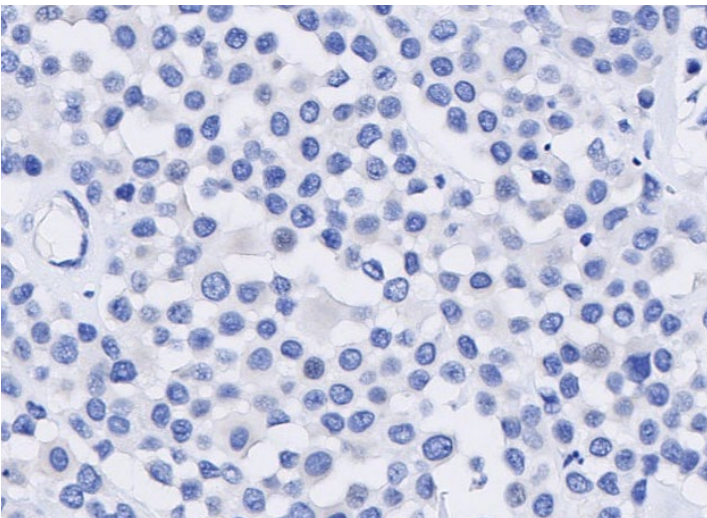
Ovarian carcinoma



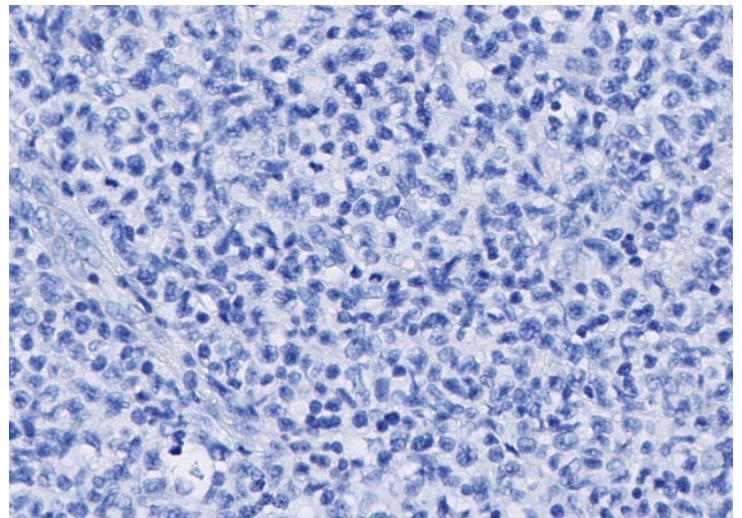
Endometrial carcinoma



Breast lobular carcinoma

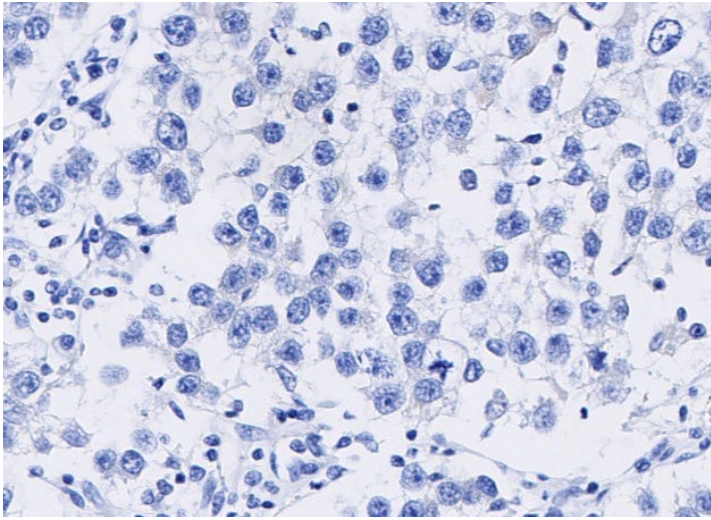


T cell lymphoma

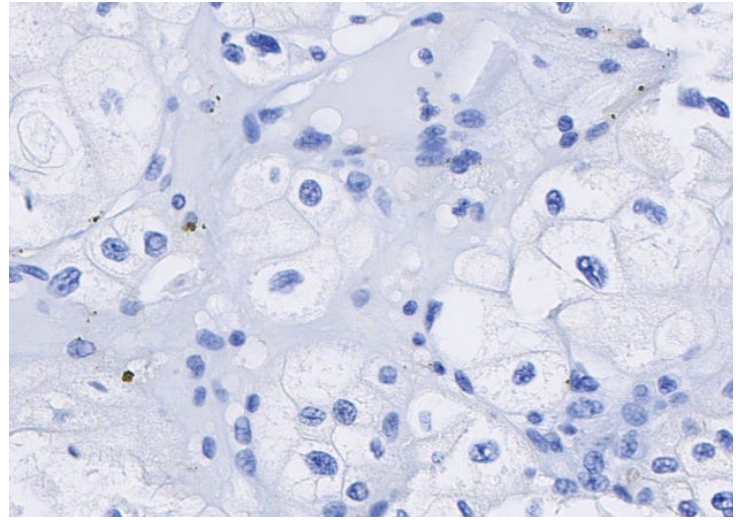


Enhanced validation data

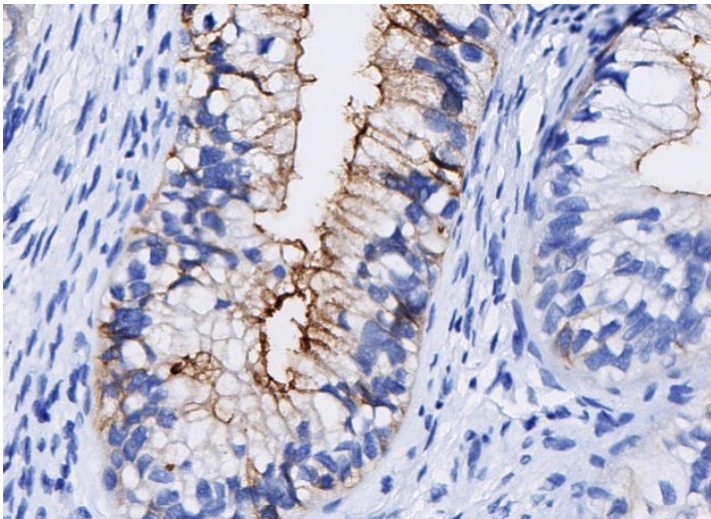
Seminoma



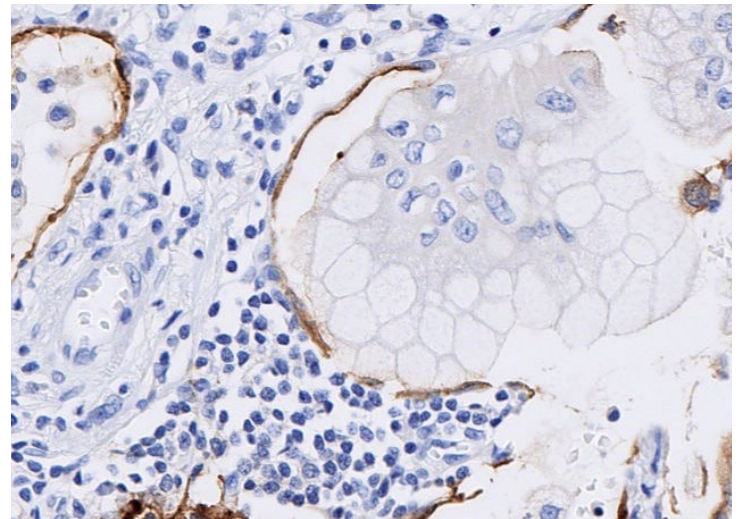
Renal cell carcinoma



Cervical cancer

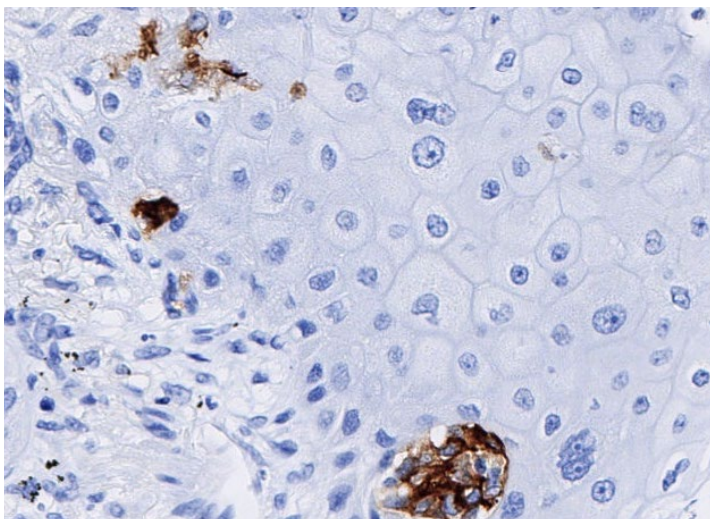


Lung adenocarcinoma

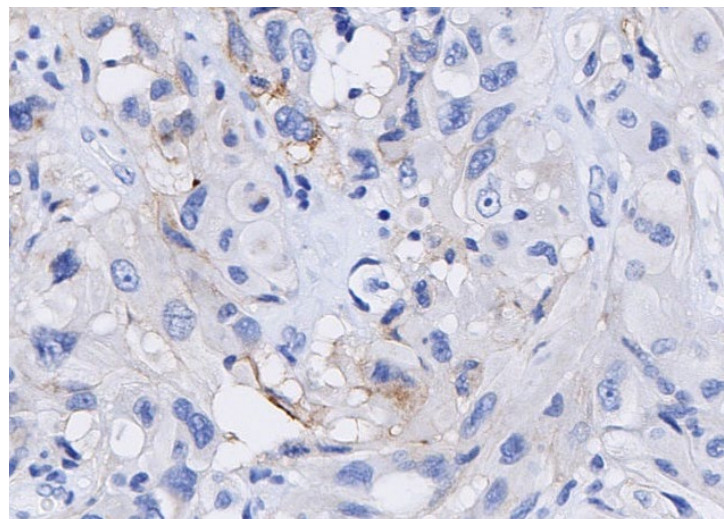


Enhanced validation data

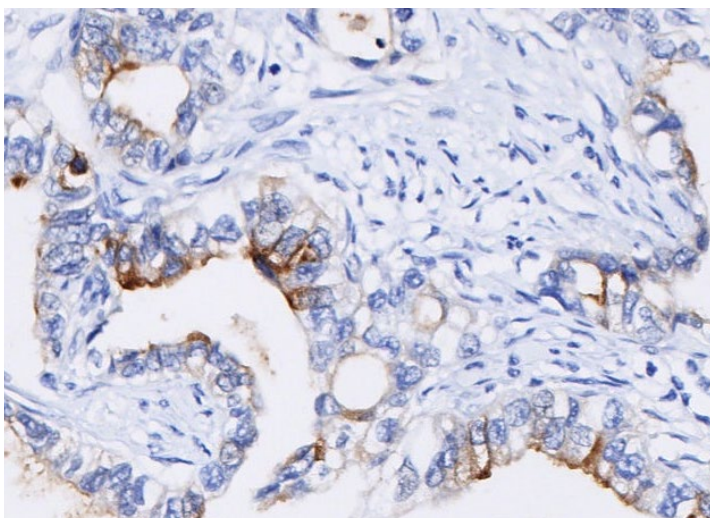
Lung squamous cell carcinoma



Glioblastoma



Stomach adenocarcinoma



Prostate adenocarcinoma

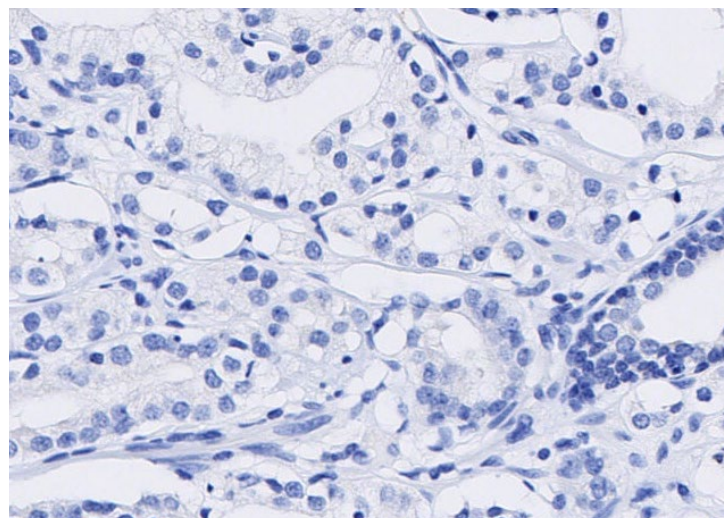
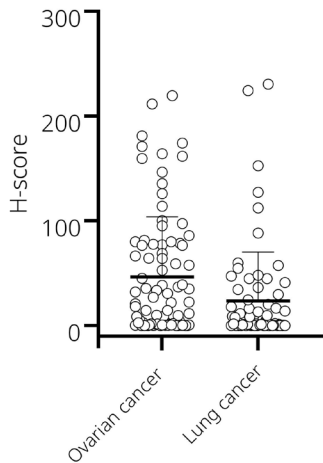


Figure 6. Folate binding protein expression in human cancer tissue. IHC staining of multi-normal human tissues using anti-folate binding protein (ab221543) (0.5ug/mL) or anti-rabbit IgG-isotype control antibody (1.0 µg/mL) (ab172730) on the Ventana DISCOVERY ULTRA platform. Positive staining in brown; nuclear hematoxylin counterstain in blue. Slides were scanned at 20x on NanoZoomer® S360 and imaged at 20X on Aperio® ImageScope.

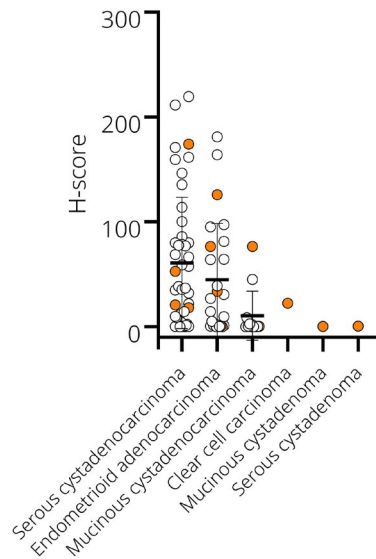
Folate binding protein expression in cancer (BOND™ RX)

Folate binding protein expression was similar in the analyzed cancer TMAs, with ovarian cancer showing marginally higher average cell membrane expression (a). The staining intensity of cohorts of cancer subtypes was also evaluated separately in scatter plots (with SD) (b-c).

a) FBP expression in selected cancer TMAs



b) FBP expression in ovarian cancer



c) FBP expression in lung cancer

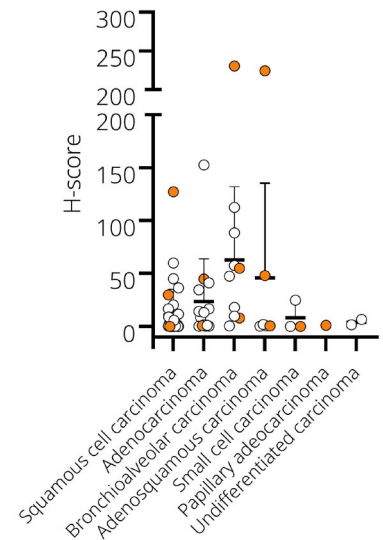


Figure 7. Folate binding protein expression in a selection of cancer TMAs.

(a) The scatter plot (with SD) summarizes H-score from cell membrane staining of folate binding protein expression in selected cancer TMA cores (ovarian cancer (85) and lung cancer (73)).

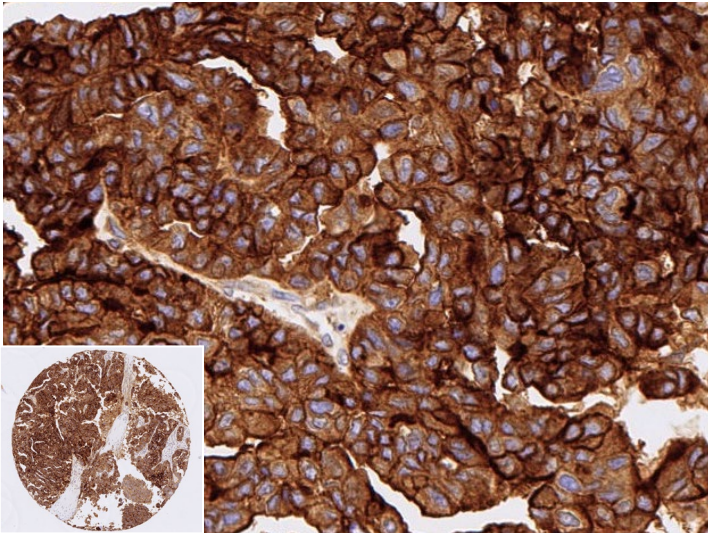
(b) H-score from cell membrane staining in 85 TMA cores/cases of ovarian cancer (serous cystadenocarcinoma (44), endometrioid adenocarcinoma (25), mucinous cystadenocarcinoma (13), clear cell carcinoma (1), mucinous cystadenoma (1), serous cystadenoma (1)). The IHC images corresponding to orange data points are shown in Figure 7.

(c) H-score from cell membrane staining in 73 TMA cores/cases of lung cancer (squamous cell carcinoma (36), adenocarcinoma (15), bronchioalveolar carcinoma (10) adenosquamous carcinoma (6), small cell carcinoma (3), papillary adenocarcinoma (1) undifferentiated carcinoma (2)). The IHC images corresponding to orange data points are shown in Figure 8.

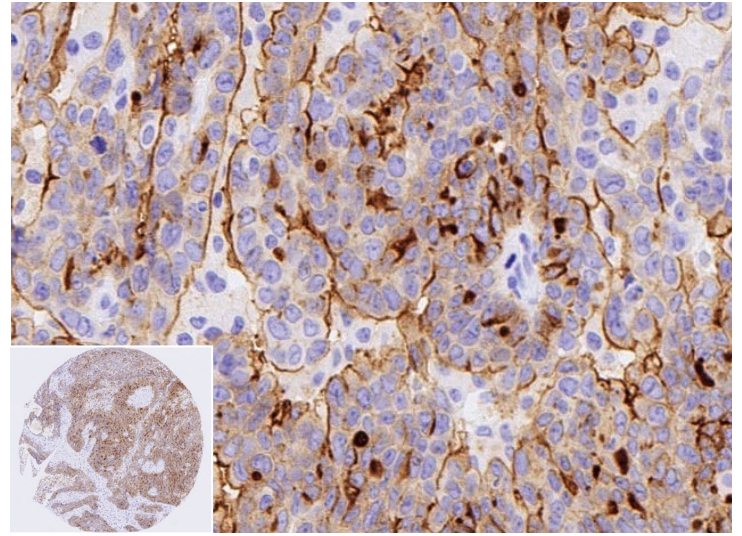
Folate binding protein expression in ovarian cancer TMA (BOND™ RX)

Below are the representative images of human ovarian cancer TMA showing strong to no expression of folate binding protein in the cell membrane.

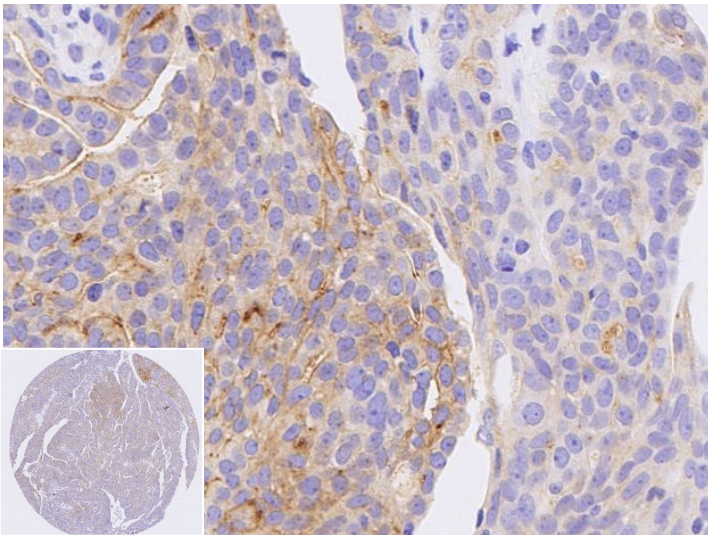
Serous cystadenocarcinoma (H-score 174.2)



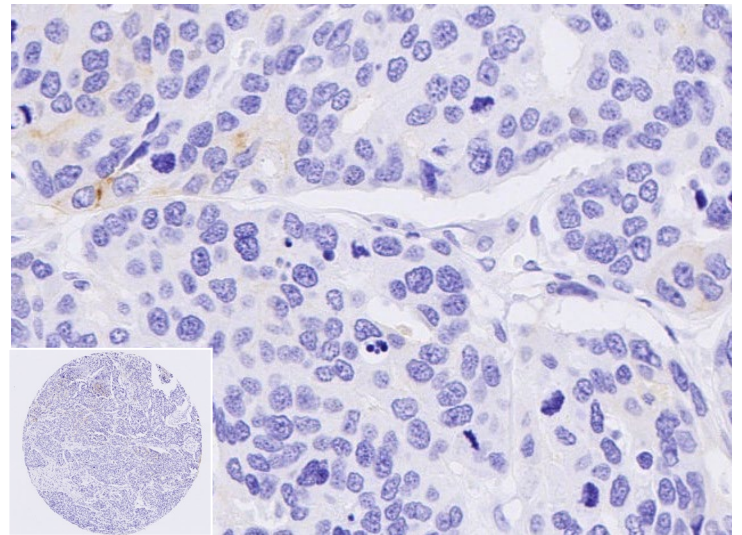
Serous cystadenocarcinoma (H-score 52.8)



Serous cystadenocarcinoma (H-score 18.2)

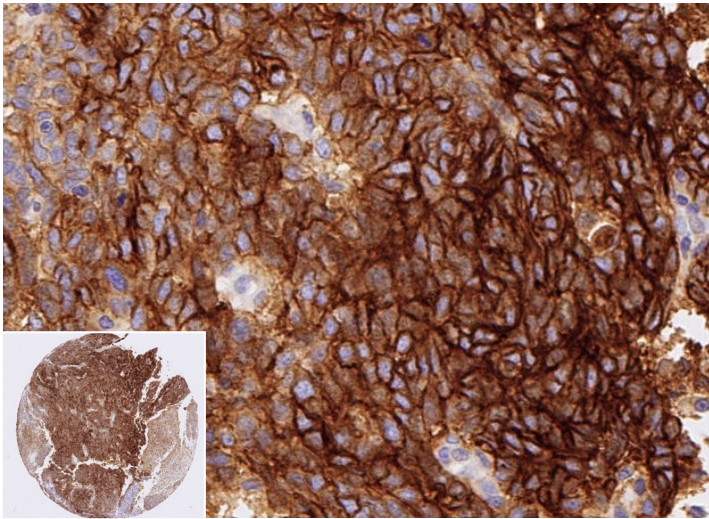


Serous cystadenocarcinoma (H-score 0.5)

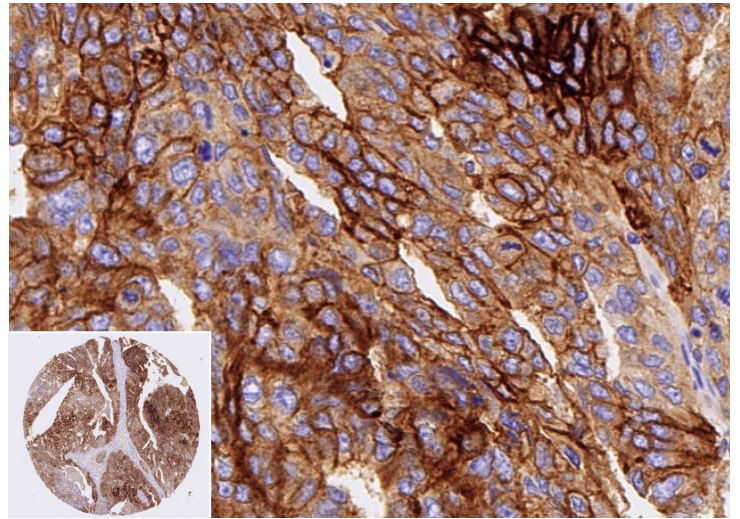


Enhanced validation data

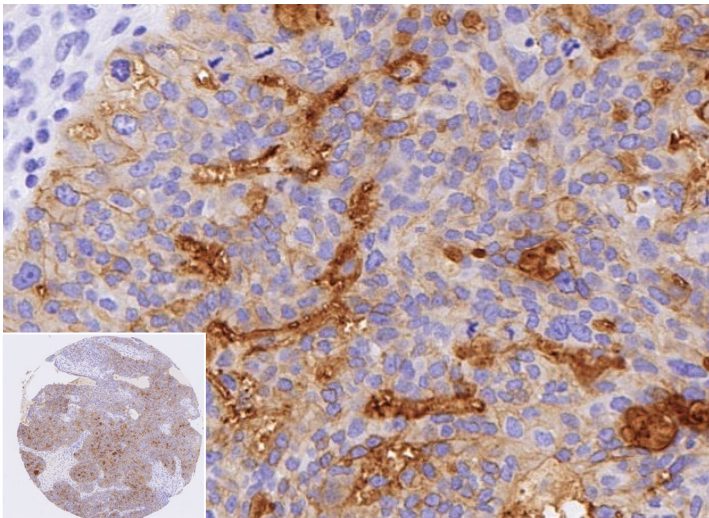
Endometrioid adenocarcinoma (H-score 126.1)



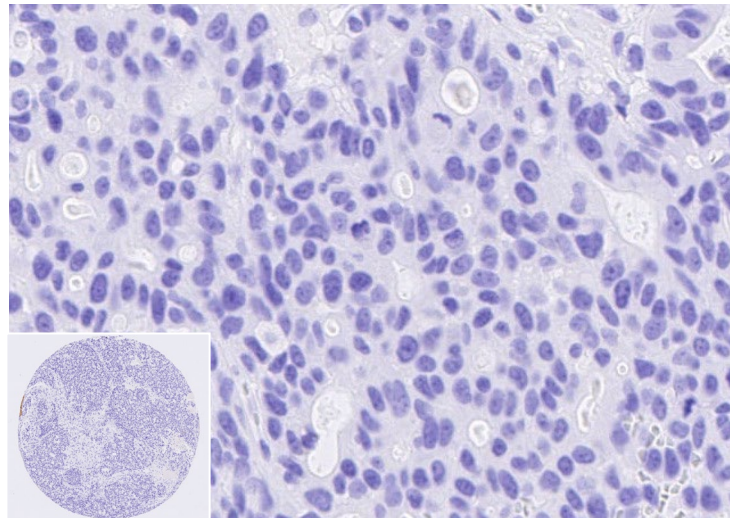
Endometrioid adenocarcinoma (H-score 76.6)



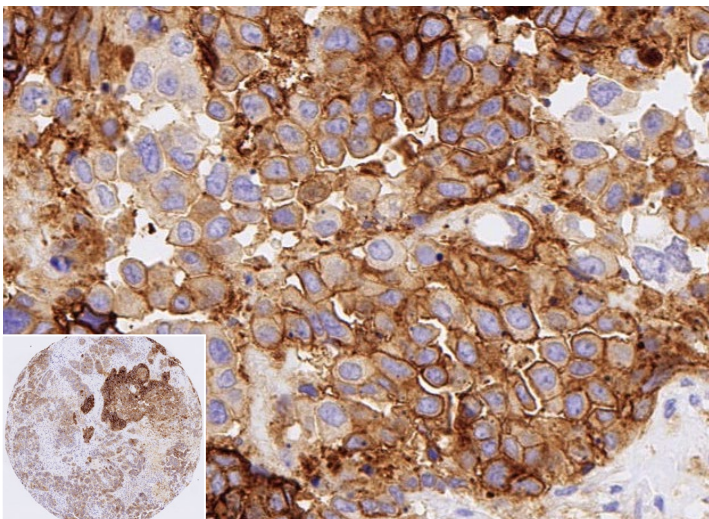
Endometrioid adenocarcinoma (H-score 33.8)



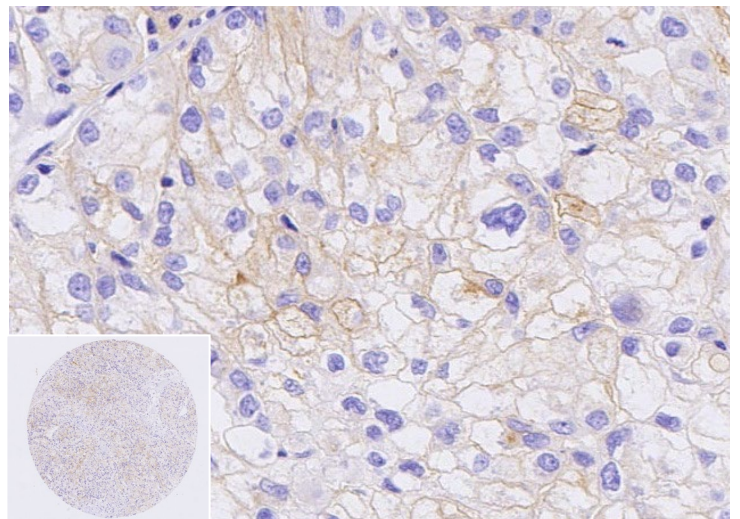
Endometrioid adenocarcinoma (H-score 0.7)



Mucinous cystadenocarcinoma (H-score 76.7)



Clear cell carcinoma (H-score 22.6)



Enhanced validation data

Mucinous cystadenoma (H-score 0.3)

Serous cystadenoma (H-score 0.7)

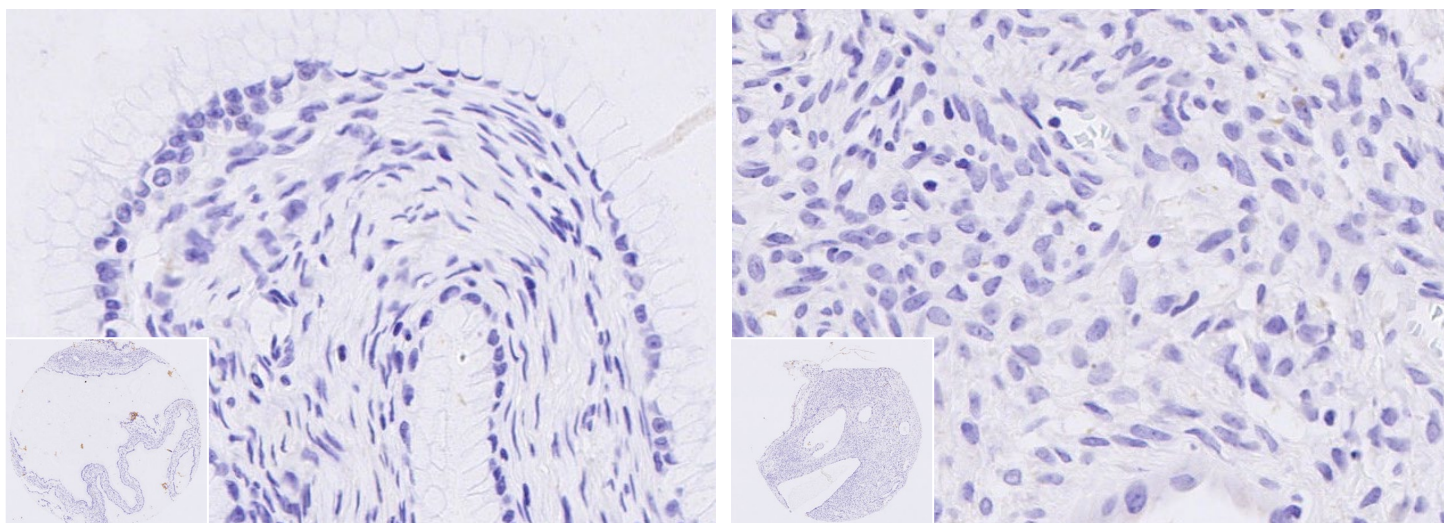
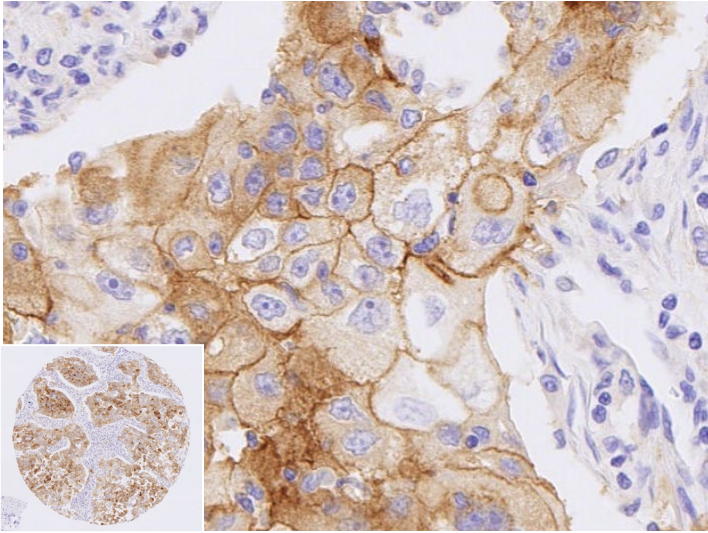


Figure 8. Folate binding protein expression in ovarian cancer. IHC images show strong, moderate and weak staining in brown; nuclear hematoxylin counterstain in blue. Slides were stained using a BOND™ RX Research Stainer (Leica®), scanned at 20x on NanoZoomer® S360 and imaged at 20x (whole core insets at 4x) on Aperio® ImageScope.

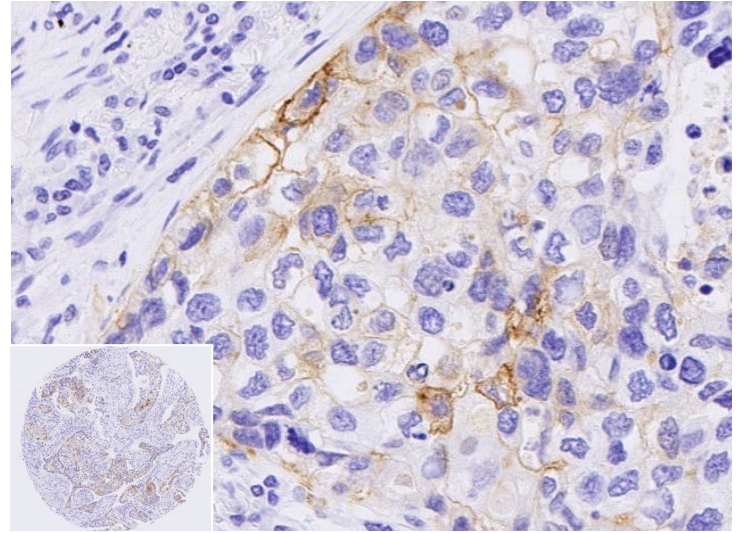
Folate binding protein expression in lung cancer TMA (BOND™ RX)

Below are the representative images of human lung cancer TMA showing strong to no expression of folate binding protein in the cell membrane.

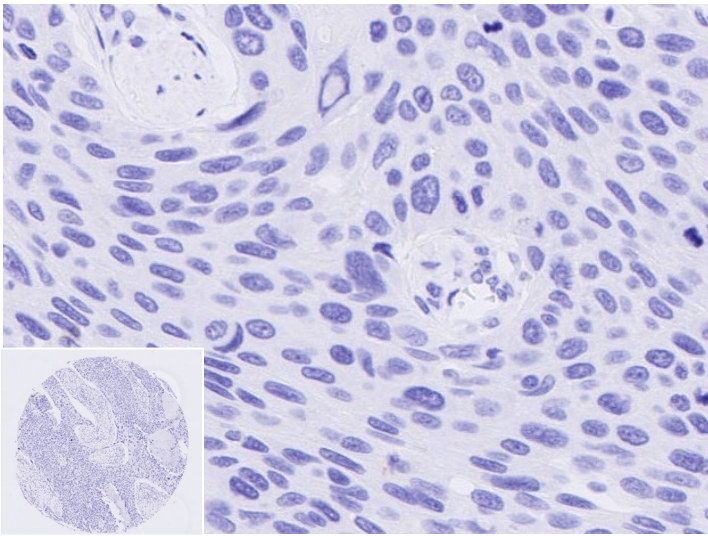
Squamous cell carcinoma (H-score 127.2)



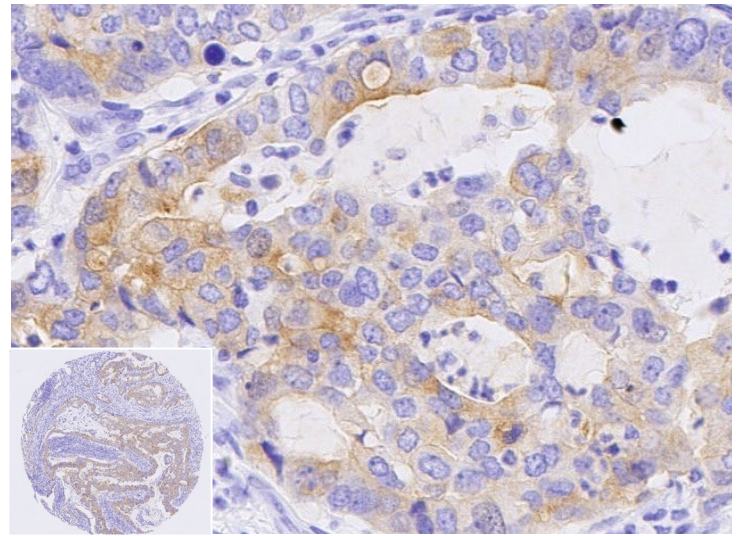
Squamous cell carcinoma (H-score 29.8)



Squamous cell carcinoma (H-score 0.0)

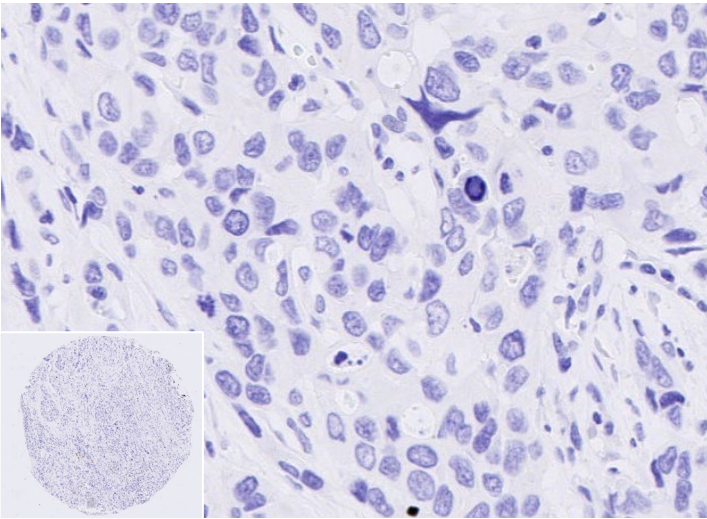


Adenocarcinoma (H-score 44.9)

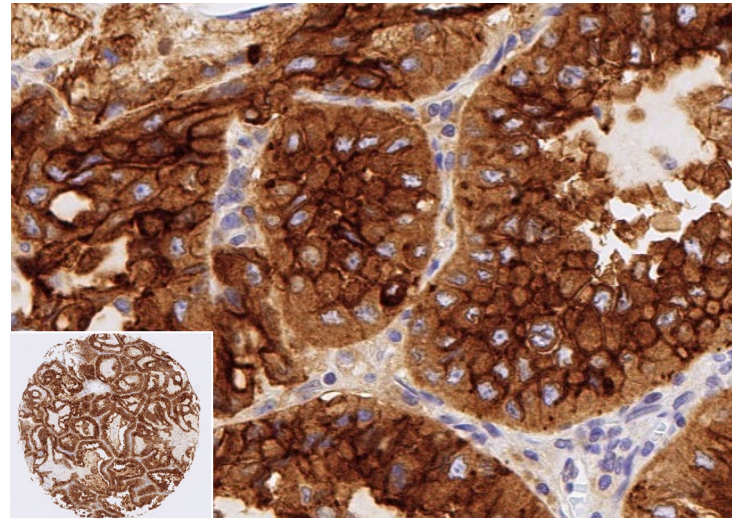


Enhanced validation data

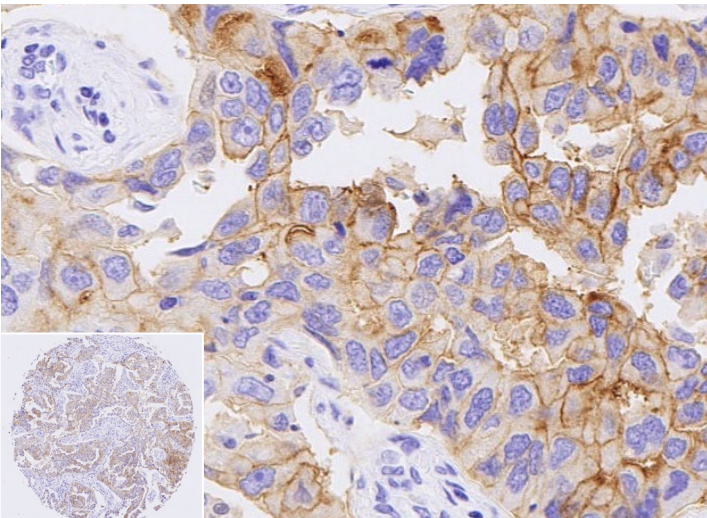
Adenocarcinoma (H-score 0.7)



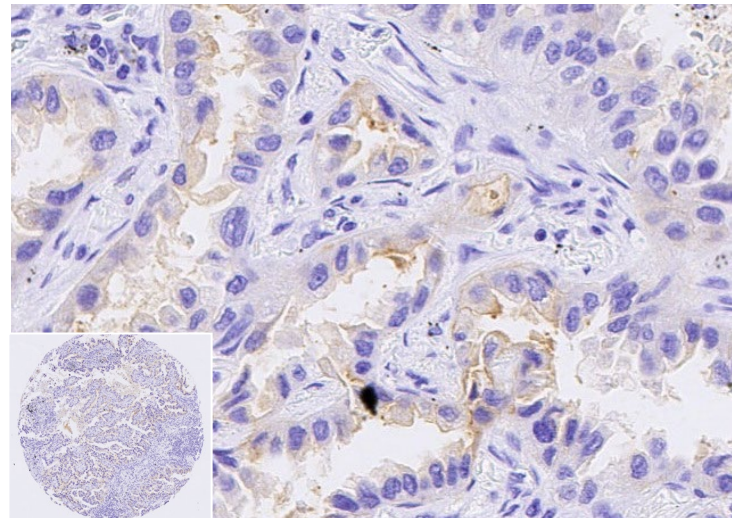
Bronchioloalveolar carcinoma (H-score 230.5)



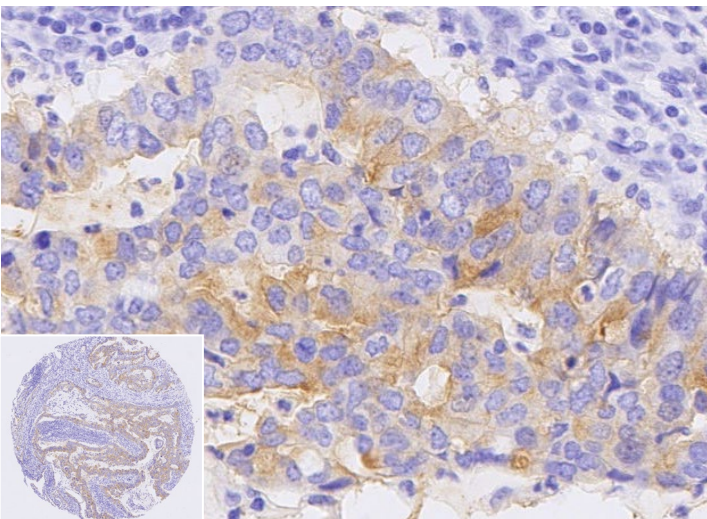
Bronchioloalveolar carcinoma (H-score 54.9)



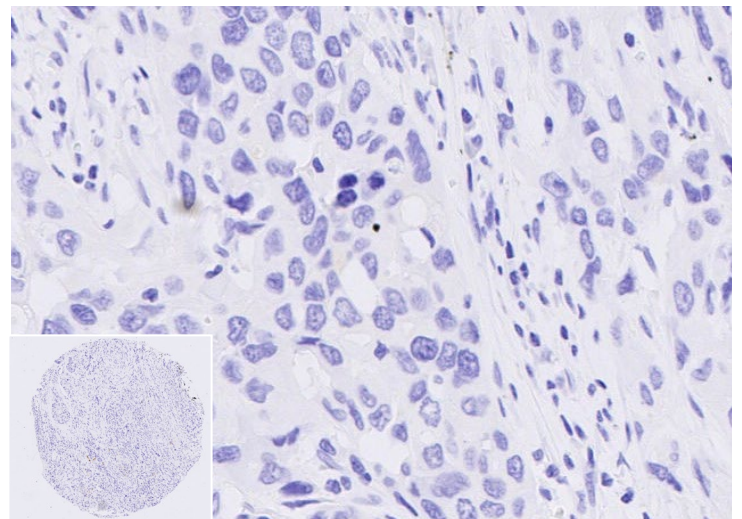
Bronchioloalveolar carcinoma (H-score 7.8)



Adenosquamous carcinoma (H-score 44.9)



Adenosquamous carcinoma (H-score 0.7)



Enhanced validation data

Small cell carcinoma (H-score 0.0)

Papillary adenocarcinoma (H-score 1.1)

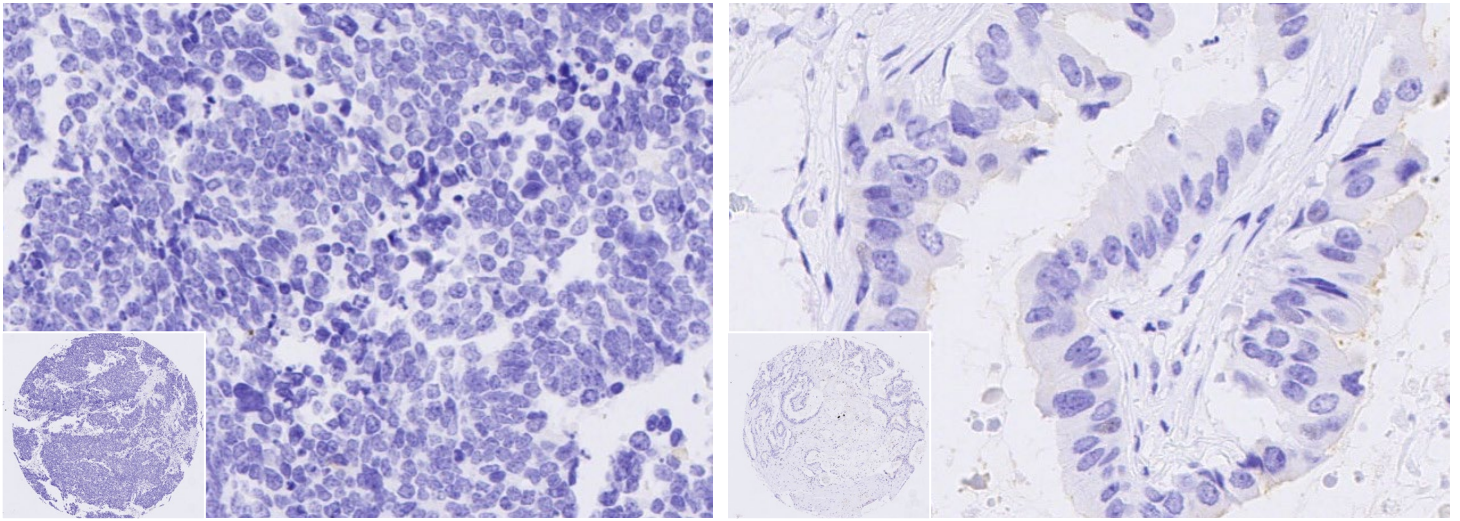


Figure 9. Folate binding protein expression in lung cancer. IHC images show strong, moderate and weak staining in brown; nuclear hematoxylin counterstain in blue. Slides were stained using a BOND™ RX Research Stainer (Leica®), scanned at 20x on NanoZoomer® S360 and imaged at 20x (whole core insets at 4x) on Aperio® ImageScope.

References

1. Zhao R, Diop-Bove N, Visentin M, Goldman ID. Mechanisms of membrane transport of folates into cells and across epithelia. *Annu Rev Nutr.* 2011 Aug 21;31:177-201. doi: 10.1146/annurev-nutr-072610-145133. PMID: 21568705; PMCID: PMC3885234.
2. Elnakat H, Ratnam M. Distribution, functionality and gene regulation of folate receptor isoforms: implications in targeted therapy. *Adv Drug Deliv Rev.* 2004 Apr 29;56(8):1067-84. doi: 10.1016/j.addr.2004.01.001. PMID: 15094207.
3. Parker N, Turk MJ, Westrick E, Lewis JD, Low PS, Leamon CP. Folate receptor expression in carcinomas and normal tissues determined by a quantitative radioligand binding assay. *Anal Biochem.* 2005 Mar 15;338(2):284-93. doi: 10.1016/j.ab.2004.12.026. PMID: 15745749.
4. Varaganti P, Buddolla V, Lakshmi BA, Kim YJ. Recent advances in using folate receptor 1 (FOLR1) for cancer diagnosis and treatment, with an emphasis on cancers that affect women. *Life Sci.* 2023 Aug 1;326:121802. doi: 10.1016/j.lfs.2023.121802. Epub 2023 May 25. PMID: 37244363.
5. Mai J, Wu L, Yang L, Sun T, Liu X, Yin R, Jiang Y, Li J, Li Q. Therapeutic strategies targeting folate receptor α for ovarian cancer. *Front Immunol.* 2023 Aug 30;14:1254532. doi: 10.3389/fimmu.2023.1254532. Erratum in: *Front Immunol.* 2024 Apr 17;15:1403324. doi: 10.3389/fimmu.2024.1403324. PMID: 37711615; PMCID: PMC10499382.
6. Bax HJ, Chauhan J, Stavrika C et al. Folate receptor alpha in ovarian cancer tissue and patient serum is associated with disease burden and treatment outcomes. *Br J Cancer.* 2023 Jan;128(2):342-353. doi: 10.1038/s41416-022-02031-x. Epub 2022 Nov 19. PMID: 36402875; PMCID: PMC9902484.
7. Scaranti M, Cojocaru E, Banerjee S, Banerji U. Exploiting the folate receptor α in oncology. *Nat Rev Clin Oncol.* 2020 Jun;17(6):349-359. doi: 10.1038/s41571-020-0339-5. Epub 2020 Mar 9. PMID: 32152484.
8. Cerami E, Gao J, Dogrusoz U, Gross BE, Sumer SO, Aksoy BA, Jacobsen A, Byrne CJ, Heuer ML, Larsson E, Antipin Y, Reva B, Goldberg AP, Sander C, Schultz N. The cBio cancer genomics portal: an open platform for exploring multidimensional cancer genomics data. *Cancer Discov.* 2012 May;2(5):401-4. doi: 10.1158/2159-8290.CD-12-0095. Erratum in: *Cancer Discov.* 2012 Oct;2(10):960. PMID: 22588877; PMCID: PMC3956037.
9. Gao J, Aksoy BA, Dogrusoz U, Dresdner G, Gross B, Sumer SO, Sun Y, Jacobsen A, Sinha R, Larsson E, Cerami E, Sander C, Schultz N. Integrative analysis of complex cancer genomics and clinical profiles using the cBioPortal. *Sci Signal.* 2013 Apr 2;6(269):pl1. doi: 10.1126/scisignal.2004088. PMID: 23550210; PMCID: PMC4160307.
10. de Bruijn I, Kundra R, Mastrogiacomo B, Tran TN, Sikina L, Mazor T, Li X, Ochoa A, Zhao G, Lai B, Abeshouse A, Baiceanu D, Ciftci E, Dogrusoz U, Dufilie A, Erkoc Z, Garcia Lara E, Fu Z, Gross B, Haynes C, Heath A, Higgins D, Jagannathan P, Kalletla K, Kumari P, Lindsay J, Lisman A, Leenknecht B, Lukasse P, Madela D, Madupuri R, van Nierop P, Plantalech O, Quach J, Resnick AC, Rodenburg SYA, Satravada BA, Schaeffer F, Sheridan R, Singh J, Sirohi R, Sumer SO, van Hagen S, Wang A, Wilson M, Zhang H, Zhu K, Rusk N, Brown S, Lavery JA, Panageas KS, Rudolph JE, LeNoue-Newton ML, Warner JL, Guo X, Hunter-Zinck H, Yu TV, Pilai S, Nichols C, Gardos SM, Philip J; AACR Project GENIE BPC Core Team, AACR Project GENIE Consortium; Kehl KL, Riely GJ, Schrag D, Lee J, Fiandalo MV, Sweeney SM, Pugh TJ, Sander C, Cerami E, Gao J, Schultz N. Analysis and Visualization of Longitudinal Genomic and Clinical Data from the AACR Project GENIE Biopharma Collaborative in cBioPortal. *Cancer Res.* 2023 Dec 1;83(23):3861-3867. doi: 10.1158/0008-5472.CAN-23-0816. PMID: 37668528; PMCID: PMC10690089.
11. Blum A, Wang P, Zenklusen JC. SnapShot: TCGA-Analyzed Tumors. *Cell.* 2018 Apr 5;173(2):530. doi: 10.1016/j.cell.2018.03.059. PMID: 29625059.

Let's work together:
Connect with us at
oncology@abcam.com



Copyright© 2025 Abcam, All rights reserved.

